UNIVERSITIY OF CALIFORNIA SAN DIEGO

Cigarette Smoke Exposure Impairs Early Stages of Muscle Regeneration Following Eccentric Exercise-Induced Muscle Injury

A thesis submitted in partial satisfaction of the requirements
for the degree of Master of Science

in

Biology

by

Nicole Stevens

Committee in charge:

Professor Michael C. Hogan, Chair
Professor Randolph Hampton, Co-chair
Professor James Kadonaga

2021

The thesis of Nicole Stevens is approved, and it is acceptable in quality and form for publication on microfilm and electronically.

University of California San Diego

2021

TABLE OF CONTENTS

LIST OF FIGURES

LIST OF ABBREVIATIONS

CS	Cigarette smoke
COPD	Chronic Obstructive Pulmonary Disease
LCP	Lengthening Contraction Procedure
EDL	Extensor Digitorum Longus
TA	Tibialis Anterior
WT	Wild Type
Pax7	Paired Box Protein 7
Pax7TdT	Pax7CreERTdTomato
EEIMI	Eccentric Exercise Induced Muscle Injury
SCs	Satellite Cells
MHC	Myosin Heavy Chain
IP	Intraperitoneal
TNF-α	Tumor Necrosis Factor-alpha

ACKNOWLEDGMENTS

I would like to acknowledge Professor Michael C. Hogan for allowing me the opportunity to be a part of the lab in order to discovery my passion for research.

I would also like to acknowledge Leo, because none of this would have been possible without the creativity of your thinking to make this project happen. I have been so blessed to work alongside a P.I. as exciting as you.

To our grant collaborators at Sanford Burnham Prebys Medical Discovery Institute in Alessandra Sacco's Lab, I am so grateful to have had the opportunity to work with both Alessandra Sacco and postdoc Mafalda Loreti. Mafalda has served as a mentor to me throughout my graduate research, I would not have been able to accomplish so much of this project if it wasn't for her outstanding guidance and support along the way.

This manuscript is coauthored with Michael C. Hogan, Leonardo Nogueira, Alessandra Sacco, and Mafalda Loreti. The thesis author was the primary author of this manuscript.

ABSTRACT OF THE THESIS

Cigarette Smoke Exposure Impairs Early Stages of Muscle Regeneration Following Eccentric Exercise-Induced Muscle Injury

by

Nicole Stevens

Master of Science in Biology

University of California San Diego, 2021

Professor Michael C. Hogan, Chair
Professor Randolph Hampton, Co-chair

Chronic smokers present lower limb muscle dysfunction prior to the onset of overt respiratory limitations. Skeletal muscle dysfunction induced by cigarette smoke (CS) includes muscle weakness, loss of muscle mass, and decreased fatigue resistance, which directly lead to exercise intolerance. Smokers and those who develop COPD have higher incidence of muscle injury and show poor muscle regenerative capacity. The mechanism by which muscle regeneration may be affected following injury in

chronic smokers is not well investigated. Therefore, we hypothesized that chronic CS exposure delays the trajectory of muscle regeneration following an eccentric exercise-induced muscle injury (EEIMI). We aim to investigate the consequences of short- (2 month) and long- (4 month) term CS exposure in mice on muscle regeneration following EEIMI via lengthening contraction procedure (LCP). Our investigation evaluated changes in ex-vivo force contractility, myofiber cross-sectional area (CSA), and the presence of central nucleated myofibers (CNM) 7 days following LCP, during the muscle reconstruction phase. We found the CS exposure leads to a small decrease in EDL force production, a reduction in myofiber CSA, and increase of CNM in injured legs, suggesting regeneration is delayed. We aimed further to investigate the time course of muscle satellite cell (SC) fusion during the regenerative process in Pax7CreERTdTomato mice to understand better the extent of damage induced by the LCP in the TA and EDL muscles. SC fusion was only detected after 5 days recovery in TA and EDL. Together, the data suggest that CS exposure delays early stages of muscle regeneration process.

INTRODUCTION

It is widely accepted that long-term smoking is the leading preventable cause of chronic obstructive pulmonary disease (COPD) (Leberl et al., 2013), an inflammatory lung disease characterized by irreversible pulmonary airflow limitation and abnormal inflammation of the lungs (Pauwels et al., 2001). More recently, research has noted the adverse extrapulmonary effects in COPD patients, specifically that of skeletal muscles as they pertain to the patient's quality of life (Barreiro & Gea, 2016).

A thorough review of the development of the extrapulmonary manifestations of COPD has found that cigarette smoke- (CS) induced skeletal muscle dysfunction is present before the onset of overt respiratory limitations (Degens et al., 2015). Skeletal muscle dysfunction induced by CS includes decreased muscle strength, muscle wasting or atrophy, and fatigue resistance, which directly reduce exercise tolerance (Degens et al., 2015). It has also been reported that COPD patients have an increased susceptibility to skeletal muscle injuries, specifically shoulder rotator cuff tears (Baumgarten et al., 2010). However, the extent to which chronic smoke exposure affects skeletal muscle dysfunction following an exercise-induced injury remains unknown, particularly in chronic smokers and COPD patients, as they are most susceptible.

In the past, multiple teams have modeled COPD in mice by investigating the effects of CS after short- and long-term daily exposure periods, ranging from 2-6 months. During this time manifestations of some pulmonary effects from CS exposure occurred before COPD was achieved. Parameters to consider include inflammatory cell counts of the lungs, the systemic inflammatory response, and the effects on lung

mechanics via pressure-volume relationship. A robust pro-inflammatory response in the lungs was observed after 2 months of CS exposure (Chan et al., 2020) without causing an effect on lung mechanics since there was no measurable change in the lung alveolar airspace at that time (Nogueira et al., 2018). In addition to the proinflammatory response in the lungs, an increase in plasma concentration of the pro-inflammatory cytokine tumor necrosis factor-alpha (TNF-α) was observed at 2 and 4 months of CS exposure (Tang et al., 2010). After 3-month nose-only CS exposure, early signs of changes in lung mechanics began to present, observable as hyperinflation of the lungs and an increase in total lung capacity. As expected, the effects on lung mechanics seen at 3-months exposure were more pronounced in the 6-month exposed mice. This was evident by an increased lung capacity visible in the pressure-volume relationship of the lungs along with significant inflammatory response measured in bronchoalveolar fluid (Rinaldi et al., 2012). Evidence from Gosker et al. 2009, found that hallmark signs of COPD, including significant pulmonary inflammation in conjunction with systemic inflammation, were achieved after 6 months of CS exposure. At this point, the lung mechanics had been significantly compromised by 6-month nose-only CS exposure. Limited airflow and significant pulmonary inflammation in conjunction with the presence of systemic inflammation meet the criteria for COPD.

In addition to the deleterious effects initiated by pulmonary inflammation, the overspill of systemic inflammation has been speculated to worsen the extrapulmonary comorbidities associated with COPD, which in turn can potentiate the morbidity of COPD patients (Barnes & Celli, 2009). Such manifestations of these extrapulmonary effects arise at various times. It is speculated that they are interrelated and multifactorial

and include body weight abnormalities and skeletal muscle dysfunction (Agustí, 2005). Effects on appetite and body weight have been seen to take place far more rapidly than the development of systemic inflammation. After an acute 4-day exposure to CS, one study found that mouse food intake was significantly reduced, and body weight was significantly decreased within the first 2 days of CS exposure (Chen et al., 2005). Studies investigating more chronic exposure periods have found that body weight gain of mice exposed to CS is inhibited after 2 months and up to 8 months of exposure, although weight changes specifically in hind limb muscles are not observed until 6 months (Krüger et al., 2015) (Gosker et al., 2009). The immediate changes in body weight are likely attributed to the significant drop in appetite, as mentioned, while the more prolonged effects on body weight from smoking come from muscle loss (Agustí, 2005). Muscles of the mouse hind limbs including the tibialis anterior (TA), extensor digitorum longus (EDL), gastrocnemius, and soleus, are of particular interest as they are more susceptible to the effects of CS and are considered locomotor muscles. This is reflected in COPD patients as they experience lower limb skeletal muscle dysfunction at a greater rate than the upper limb and respiratory muscles (Barreiro & Gea, 2016). For this project, we will focus on mouse hind limbs.

Reduced exercise capacity and decreased fatigue resistance are common ailments of COPD patients (Barreiro & Gea, 2016). Research has shown that asymptomatic smokers often complain of fatigue during exercise and show exercise intolerance. This has been observed even before the onset of overt pulmonary symptoms, suggesting a connection between smoking and exercise intolerance (CheungID et al., 2020). As a way of determining cardiorespiratory and metabolic

health, and physical endurance fitness, maximum endurance exercise capacity is evaluated by VO2 max which measures the maximum rate of oxygen consumption during progressive intensity exercise (CheungID et al., 2020). One study finds a significant reduction in VO2 max starting at 4 months exposure; the reduction becomes more prominent in 6- and 8-month smoke exposed mice (Krüger et al., 2015). Physical endurance as measured by treadmill test was significantly reduced after 4-months smoke exposure, and evaluation of ex-vivo isolated soleus force contractility data showed decreased fatigue resistance. Analysis from the same study found no changes in EDL muscle fatigability at either 2 and 4-months CS exposure (Tang et al., 2010). Hind limb (in mice) and lower limb (in humans) skeletal muscle dysfunction have been speculated to be the main contributing factor of reduced exercise capacity and thought to be strongly correlated to the re-distribution of muscle fiber types and muscle fiber atrophy seen particularly in the locomotor muscles (CheungID et al., 2020) (Joaquim et al., 2015). Effects on muscle force contractility found no changes in the EDL and soleus muscles of mouse hind limbs after 3-months CS exposure. However, a decrease in force production of the soleus muscle was observed after 6-months exposure. This study attributed the lack of change in force production observed in the EDL muscle after 6-months exposure to the muscle fiber type composition (Krüger et al., 2015).

Fiber type composition plays a key role in the muscle's' function. Studies investigating the effects of CS on muscles often yield varying results depending on muscle fiber type composition. Skeletal muscle fibers are classified into two general groups: "slow-twitch" (type 1) and "fast-twitch" (type 2). Within the fast-twitch fiber classification there are three major subtypes; type 2A, 2B, and 2X, based on their

expression of myosin heavy chain (MHC). Classification of muscle fibers can also be based on the metabolic pathway used for energy production and muscle contraction speed. Fiber types 1 and 2A use mostly oxidative metabolism, while fiber types 2B and 2X rely mostly on glycolytic metabolism. Varying combinations of these fiber types comprise mammalian skeletal muscles, which have an effect on the muscle's functionality (Talbot & Maves, 2016). For example, fiber types of skeletal muscle in wild-type (C57BL6J) mice shows that the soleus consists of type 1 (37%) and 2A (38%) fibers, whereas the EDL, TA, and gastrocnemius consist mostly of type 2B, 66%, 60% and 54%, respectively (Augusto et al., 2004). The proportions of these fiber type compositions are plastic, meaning they are able to alter their metabolic state in order to adapt to different functions; this influences the muscles' susceptibility to muscle dysfunction (Talbot & Maves, 2016). A change in fiber type proportions, from slow-twitch to fast-twitch, is often seen in COPD patients; this is similar to changes observed in muscle inactivity disorders. Such changes in fiber type composition, specifically of the lower limbs, is strongly associated with disease severity (Talbot & Maves, 2016). Changes in fiber type proportions, from type 2a to type 2b, are detected in the soleus muscle after 2-months of CS exposure and more pronounced after 4-months, while there are no changes detected in the EDL at this time (Tang et al., 2010). Skeletal muscle fiber type can play an important role in the susceptibility or resistance in the presence of a disease. It remains unclear why certain fiber types are more or less susceptible to certain diseases (Talbot & Maves, 2016).

Other than the changes in muscle contractile function and fiber type composition observed from smoking, evidence suggest that CS exposure may have an effect on the

muscles' ability to repair following injury. Currently, there is little research on muscle regeneration following CS exposure. The only other study that was recently published on this matter finds that 2 months of CS exposure exacerbates barium chloride- ($BaCl_2$) induced skeletal muscle injury. However, the authors found that CS exposure does not seem to compromise late-stage regenerative capacity in mice. This was evident by restored in-situ TA muscle force production and partially recovered myofiber CSA of injured muscle in CS, when compared to air exposed mice (Chan et al., 2020). Conclusions were based on status of the muscle after 14 or more days of recovery. Muscle stem cell activation, however, was significantly reduced within the first 7 days in the CS exposed mice group, suggesting there was a negative impact from CS exposure on early-stage muscle regeneration (Chan et al., 2020). Previous research done in our lab suggested a correlation between muscular devascularization and a decrease in the amount of quiescent satellite cells (SCs) available around the myofibers, when mice were exposed for 2 months (Nogueira et al., 2018). Based on this conclusion, we speculated that CS exposure would impair the muscles' ability to recovery from an injury.

When considering any study looking at muscle regeneration it is important to examine the way in which the muscle was damaged, as it will impact the trajectory of the regenerative process (Hardy et al., 2016). Typically, skeletal muscle injury is defined by physiological or morphological changes which are commonly expressed by quantitative analysis of decrements in force production or measurable architectural disruptions of the myofiber (Tidball, 2011). The most commonly used injury models in research include injections of toxins such as: Cardiotoxin (CTX), Notexin (NTX), and

BaCl2 (Hardy et al., 2016). The latter was used in the above study (Chan et al., 2020). The main caveat to using toxins is the likelihood of the toxins having unknown effects on the other cells playing a role in the regenerative process (Hardy et al., 2016). Alternative methods of damage include crushing or freezing the muscle, imposing denervation or devascularization of the muscle, or subjecting the muscles to repeated bouts of eccentric exercise thus causing an eccentric exercise induced muscle injury (EEIMI) (Chargé & Rudnicki, 2004). The only physiologically relevant model of damage is the EEIMI, which is usually produced by imposing lengthening contractions on locomotor muscles (Chargé & Rudnicki, 2004) as it closely resembles the most commonly seen muscle injury (Dueweke et al., 2017). Such encounters with eccentric exercise that commonly occur involve the transition from sitting to standing and downhill walking or running (Lovering & Brooks, 2014) (Vogt & Hoppeler, 2014). Before we can explore the effects of CS on muscle regeneration following a muscle injury, we need to identify the key features of the regeneration process. Muscle regeneration can be separated into 5 distinct yet interrelated and time dependent phases: degeneration accompanied by inflammation, reconstruction, maturation, and functional recovery. While these phases can overlap and occur at differing time points depending on the intensity of damage induced, they are distinguishable by cellular and molecular markers (Forcina et al., 2020). It has been hypothesized that damage to the lining of the myofiber, sarcolemma, results in an influx of calcium to the myofiber thus causing calcium-dependent proteolysis which initiates the tissue degeneration process (Chargé & Rudnicki, 2004). This is followed by infiltration of various inflammatory cells that

will cause a cascade of inflammatory cytokines, which occurs at site of injury (Forcina et al., 2020).

The early stages of muscle regeneration, following degeneration, are usually accompanied by a well-orchestrated and highly regulated inflammatory response involving multiple cell types, which leads to the activation and recruitment of muscle stem cells, known as satellite cells (SCs) (Gardner et al., 2020). Reconstruction of injured muscle tissue relies on these SCs. SCs, first detected by Dr. Alexander Mauro (Rockefeller Institute) (Mauro, 1961) were named based on their location as they reside between the basal lamina and sarcolemma surrounding the muscle fiber (Musarò, 2014) and are within close proximity to blood vessels (Christov et al., 2007). Under homeostatic conditions, SCs remain in a quiescent state until activated by muscle damage (Forcina et al., 2020). These cells can be detected by the expression of paired box protein 7 (Pax7), a common marker of quiescent and committed SCs. After an injury, activated SCs migrate towards site of injury and re-enter the cell cycle to begin proliferation. At this point, SCs undergo cell divisions to differentiate, in an effort to recover damaged tissue or self-renew, thereby returning to quiescence to replenish their cell pool for later use (Dumont et al., 2015). Following the proliferative phase, the SCs that are prompted to become committed will differentiate and become myoblasts. At this stage, the myogenic marker MyoD is highly expressed, while Pax7 is under-expressed. Myoblasts can either fuse with existing myofibers to repair damaged myofibers, or fuse together and form new myofibers (Järvinen et al., 2008). Within 5-6 days following an exercise- induced injury, the degenerated portion of the myofiber will have been replaced by a newly formed or repaired myofibers (Järvinen et al., 2008). A

hallmark for this phase of regeneration is the presence of centrally located nuclei within the myofiber (Forcina et al., 2020). This is a sign that the repair phase of muscle regeneration is ending and that continued growth and remodeling phase are taking place.

The later stages of muscle regeneration involve maturation and remodeling of the myofibers. Myofiber maturation often peaks around 7 days post-injury and is observable by structural remodeling and growth of the muscle fibers, as outlined in Figure 1. This can be measured by the change in the cross-sectional area (CSA) of the myofiber at different time points throughout the recovery process. Efficient muscle regeneration can be confirmed by the maturation of newly formed fibers as well as fully repaired damaged fibers; this phase is known to be complete when centralized nuclei of damaged fibers have returned to their periphery. Lastly, the healing process as a whole is complete once the muscle has fully regained functionality, often measured by contractile function of the muscle (Forcina et al., 2020).

Previous research on the effects of CS during muscle repair have not imposed a physiologically relevant method of damage that is analogous to what an injury prone chronic smoker or COPD patient would likely endure. Hence, it is imperative to understand the effects of CS on muscle repair, particularly in COPD patients who are more susceptible to these injuries. We hypothesized that CS exposure impairs the early stages of muscle regeneration after EEIMI. Therefore, the aim of this study is to investigate whether CS has an effect on muscle repair in mouse hind limb skeletal muscles, specifically the anterior crural muscles, which consist of the TA and EDL, before overt respiratory symptoms occur. Our study is the first to implement an EEIMI,

using a lengthening contraction procedure (LCP), to investigate the effects of CS exposure in a pre-COPD mouse model 7 days after injury. To understand further what is occurring during the healing process following the EEIMI, transgenic Pax7CreERTdTomato (Pax7TdT) mice were used to study the activation and fusion of SCs into myofibers 3-, 5-, and 7-days post-injury. Our evaluation of the effects of CS following injury included ex-vivo force contractility data obtained from the EDL and histological analysis of the TA. These measurements were also obtained from the Pax7TdT mice, in addition to histological analysis of the EDL. Together, the data from the Pax7TdT mice, were used to establish a relationship between the extent of the injury induced by the LCP in both TA and EDL muscles and to analyze the regeneration process. This process allowed us to evaluate the intensity of muscle damage that occurred in EDL and TA muscles from the Air of CS exposed mice.

RESULTS

Young adult mice, ages 7-8 weeks, were used to investigate the effects of cigarette smoke (CS) on muscle repair. To do so, mice were separated into two main categories: Air exposed (negative control), and CS exposed (12 mice each) (Fig. 2). One group of mice consisting of these two categories was exposed for 2 months, while another group was exposed for 4 months. Within these Air or CS exposed groups, the right legs of all mice were subjected to an eccentric exercise-induced muscle injury (EEIMI) using a lengthening contraction procedure (LCP) one week before the end of their exposure periods, and the left leg served as the uninjured contralateral control leg. During the one-week recovery period these mice continued their exposure to Air or CS.

The present study examined the effects of CS in a pre-COPD mouse model. First, CS exposure in mice was validated and lung mechanics were measured, then systemic effects were measured by changes in body weight, and changes in muscle physiology following an exercise-induced injury were investigated. Transgenic Pax7TdT mice were used to provide more information during the one-week recovery process and to serve as a comparable model for the Air and CS exposed mice as they underwent the same injury procedure (Fig. 3).

Assessment of Cigarette Smoke Delivery

To start, we confirmed exposure to CS in mice by measuring the concentration of cotinine in the plasma of the 4-month exposed mice. Cotinine is a nicotine metabolism by-product and is the most validated and reliable indicator of tobacco cigarette smoke exposure (Matsumoto et al., 2010). The cotinine assay reveals that the

CS exposed mice (0.439±0.008 ng/mL) express a significantly higher amount of cotinine than the Air exposed mice (0.018±0.008 ng/mL) ($P<0.0001$, t-test) (Fig. 4A). Our lab has previously shown that after 2 months of nose-only CS exposure there is a significant increase in plasma cotinine levels compared to Air exposed control mice (Nogueira et al., 2018). As expected, our data reflect a significant increase in the plasma cotinine levels measured from the 4-month CS exposed mice.

Pressure-volume relationship of the lungs provide context in the development of the pulmonary effects seen in COPD patients. We analyzed the effects of CS on lung mechanics between the 4-month Air and CS exposed mice. We were able to collect data of the PV lung mechanics in 11 Air mice and 8 CS mice. As expected, CS mice showed a significant increase in lung volumes ($P<0.0001$, Two-way ANOVA, Bonferroni post-test) vs. Air exposed mice (Fig. 4B).

Effects of Cigarette Smoke Exposure on Body Weight

It has been previously shown that CS exposure has a significant effect on body weight gain in mice (Talukder et al., 2011). It is well recognized that smoke exposure is associated with weight loss, as seen in the many models of COPD in mice which have shown weight gain attenuation (Talukder et al., 2011). Both groups, Air and CS mice, of the 2- or 4-month exposure periods, started with similar average body weights before beginning exposure. The starting average weight of the 4-month Air exposed mice was 9.23, or ±0.62% more than the 2-month Air exposed mice, and the 4-month CS exposed mice weighed 12.3, or ±0.53% more than the 2-month CS exposed mice. These differences are not statistically significant. Mouse body weight, measured before exposure period and on last day of exposure period, seen in Fig. 5A, indicate that both

Air and CS mice of the 2-month exposure group show significant weight gained throughout the exposure (Air initial 24.3±0.65g, final 27.3±0.59g and CS initial 24.3±0.49g, final 26.3±0.44g). The 4-month Air exposed mice also show significant weight gained (Air initial 26.8±0.58g, final 28.5±0.62g), analysis done by paired t-test ($P<0.05$). The 4-month CS exposed mice, however, did not gain a significant amount of weight throughout the 4-month exposure period (CS initial 27.7±0.57g, final 28.3± 0.54g). The pattern of body weight changes throughout the 4-month exposure period, as measured on a weekly basis, Fig. 5B, reveals that both Air and CS mice experienced an immediate drop in weight gain (Air –0.36± 0.15g, and CS –0.60± 0.14g) within the first week of the exposure period. A second drop in weight gain was seen on the last week of the exposure period, in the Air and CS exposed mice of the 4-month group (1.78± 0.35g and 0.61± 0.34g, respectively). The 2-month Air and CS exposure mice showed no significant differences in body weight gain (Air 2.98±0.38g and CS 1.97±0.47g). Mouse body weight gain of the 4-month exposure group shows significantly less weight gained by CS mice (0.98±0.30g) when compared to the Air exposed mice (1.88±0.36g) (Fig. 5C).

EDL Muscle Morphometrics and Force Development

We next assessed whether CS exposure affects muscle repair. First, we analyzed the weight of mouse hindlimb muscle, EDL, without (control leg) or with injury (LCP leg). EDL muscle mass of the 2-month Air and CS exposed mice showed no significant differences between the Control (Air 12.79± 0.37mg, and CS 12.47± 0.39mg) or LCP (Air 12.28±0.38mg, and CS 12.79±0.45mg) leg EDL muscles. In contrast the 4-month exposed group showed significant decrease in EDL mass in the LCP leg of CS exposed

mice (Air Control 13.61± 0.39mg, Air LCP 12.49± 0.6mg, and CS Control 13.31± 0.36mg, CS LCP 11.84± 0.59mg). The cross-sectional area (CSA) of the whole EDL muscle is calculated using the muscle mass and muscle length. There is no significant difference in EDL CSA of the 2-month Air or CS exposed groups between the Control and LCP legs (Air Control 0.887± 0.02 mm^2 and LCP 0.848±0.02 mm^2, and CS Control 0.865± 0.02 mm2 and LCP 0.919± 0.02 mm^2); however, there is a significant decrease in the LCP legs of the 4-month Air and CS EDL muscles (Air Control 0.943±0.02 mm^2 and LCP 0.841±0.03 mm^2, and CS Control 0.909±0.02 mm2 and LCP 0.786±0.03 mm^2) (Fig. 5E).

During the muscle injury procedure, torque production of the anterior crural muscles, consisting of the TA and EDL, was measured to confirm decrease in torque. Gradual decrease in peak isometric torque measurements throughout the LCP procedure showed that the initial contractions of the Air and CS mice (Air 2.94± 0.35n* mm^2 and CS 2.86± 0.13n* mm^2) decreased by 71.3±4.5% and 70.2±3.9%, respectively, by the last (150th) contraction of the procedure (Fig 6B). During the one-week recovery period mice continued Air or CS exposure before EDL muscles were isolated to test force development during ex-vivo electrical stimulations. Force development of the EDL in the 2-month Air exposed mice reached a peak of 473.16±25 kPa for the Control leg and 443.41± 24 kPa for the LCP leg (Fig. 7A). The 2-month CS exposed mice reached a peak of 468.79±13 kPa for the Control leg and the LCP leg produces significantly less force of 398.53±24 kPa (Fig. 7B). Comparison between the Control legs of the 2-month Air and CS exposed mice shows no significant differences in EDL force production (Fig. 7C), while the LCP legs show that the CS exposed EDL muscle produced

significantly less force than the Air exposed LCP leg tested by Two-way ANOVA ($P<0.05$) (Fig. 7D). Maximum force production of the EDL in the Control legs of the 4-month Air exposed mice reached 396.51±19 kPa, while the LCP leg reached a peak of 343.62±27 kPa (Fig. 7E). The 4-month CS exposed mice produced peak force at 416.89±26 kPa in the Control leg EDL and 352.48±24 kPa in the LCP leg EDL (Fig. 7F). Comparison of force development of the 4-month exposed Control legs reveals that the Air exposed mice produced less force than the CS exposed mice tested by Two-way ANOVA ($P<0.01$) (Fig. 7G), and the LCP legs of the 4-month Air and CS exposed mice show no difference in EDL force production (Fig. 7H). Although not statistically significant, it is important to note that the averaged maximum isometric force produced in the Control leg EDL of the 4-month Air exposed mice was 16.2% less than the peak force of the 2-month Air exposed Control leg, and the 4-month Air LCP leg produced 22.5% less force than the 2-month Air LCP leg. The same was true for the CS exposed mice force production: 4-month Control leg produced 11.1% less force, while the LCP leg also produced 11.6% less force when compared to the 2-month exposed EDL force production.

TA Histological Analysis

The effects of CS on muscle repair were also investigated via histological analysis of the primary anterior crural muscle, the Tibialis anterior (TA), from the 4-month Air and CS Exposed mice groups 7-days post injury. To do this, we performed an immunostaining using anti-Laminin antibody (myofiber basal lamina marker) to analyze the cross-sectional area (CSA) of the myofibers and DAPI, a marker for nuclei,

to count central nucleated myofibers. The immunostaining of the Control leg showed signs of a healthy muscle, with muscle fibers uniform in size and with peripherally located nuclei. Damage induced by the LCP was visible by irregularly shaped myofibers and many central nuclei+ myofibers (Fig. 8A, B). The average myofiber CSA of the LCP legs were significantly smaller in both Air (1524.80±96 μm^2) and CS (1235.16±50 μm^2) mice, when compared to control legs, with the CSA of the CS LCP leg 19% lower than the Air LCP leg. The Control legs (Air 1791.8± 45μm^2 and CS 1775.2± 71 μm^2) had no significant difference in average myofiber CSA between each other (Fig. 9A). The distribution of myofiber CSA in the Control legs of both Air and CS mice showed no significant difference. Distribution of CSA in the LCP legs of both Air and CS groups displayed a notable increase in percentage of myofibers in categories below 1000 μm^2, with the highest increase in the CS exposed LCP leg myofibers ($P<0.05$, Two-way ANOVA) (Fig. 9C). Central nuclei+ myofibers were seen in significantly higher levels in the LCP leg of the CS exposed mice (27.47±5.2%, $P<0.05$, t-test) than in the Air exposed mice (13.8± 3.8%) (Fig. 9D). The percentage of the central nuclei myofibers revealed that the CS exposed mice had a significantly higher percentage of centered nuclei myofibers ($P<0.01$, two-way ANOVA) in the CS LCP leg compared to the Air LCP legs (Fig. 9E). An immunofluorescent staining of the TA muscles at 7-day post-LCP highlighted any structural changes, consisting of changes in myofiber CSA and central nucleated myofibers between the Control and LCP TA muscles.

Pax7TdT Mice EDL Force Development

To further investigate the regenerative process of the muscles during the first 7 days of recovery, Pax7TdT mice were split into three groups: 3, 5, 7-days post-injury (n=3 per group) to analyze the incorporation of Pax7+ cells into myofibers. These mice were all subjected to the same LCP procedure as the Air and CS exposed mice and showed the same trend of decreased isometric torque development (3-Day 79.2%, 5-Day 82.1%, and 7-Day 80.1% decrease) of the anterior crural muscles during the LCP procedure (Fig. 10). Muscle functionality was also assessed in isolated ex-vivo EDL muscles via isometric force development in 3, 5, 7-days post-LCP. The force produced by the LCP legs for each group was normalized to the maximum force produced by the contralateral Control leg. Force development of the EDL shows that the LCP legs produced more force with days recovered and that there were significant differences in recovery of the LCP force from days 3 to 7 ($P<0.05$) and days 5 to 7 ($P<0.05$) tested by Two-way ANOVA (Fig. 11). Maximum tetanic force developed by the EDL in the Control and LCP legs were as follows: 3-Day Control 331.8± 13 kPa and LCP 255.6± 32 kPa, 5-Day Control 470.61± 15 kPa and LCP 283.5± 48 kPa, and 7-Day Control 412.4± 58 kPa and LCP 305.9± 35 kPa.

Pax7TdT Histological Analysis

Immunofluorescent staining of the TA and EDL muscles from the Pax7TdT mice highlighted the changes in muscle morphology of the Control and LCP legs throughout the 3-day, 5-day, and 7-day recovery process (Fig. 12). Changes in myofiber CSA in both TA and EDL muscles showed that the LCP legs had a higher percentage of

myofibers with smaller CSA, most notably in the TA of the 5-day and 7-day post-LCP groups, and in the EDL of the 3-day and 5-day post-LCP groups tested by two-way ANOVA $P<0.05$ vs Control leg (Fig. 13). The percentage of TdT positive myofibers was significantly higher in the 5-day (Control 2.23±1.9, LCP 16.56±3.4) and 7-day (Control 1.31±0.9, LCP 26.2±2.8) LCP legs of the TA when compared to the Control legs, ($P<0.05$, Two-way ANOVA) (Fig. 14C). The percentage of TdT positive myofibers in the EDL of the 7-day LCP leg (18.44 ±2.8) was significantly higher when compared to the 3- and 5-day groups LCP legs($P<0.05$, Two-way ANOVA) (Fig. 11D). When looking at the CSA distribution of the TdT positive myofibers in the LCP legs of the TA it is clear that the 5-day and 7-day groups of mice had a significantly higher percentage of TdT positive fibers in smaller CSA than the 3-day TA LCP muscle ($P<0.05$, Two-way ANOVA, Bonferroni Post-test) (Fig. 14E). It can also be seen that the CSA distribution of the TdT positive myofibers in the EDL were significantly higher in the 7-day group of mice when compared to the 3 and 5-day groups ($P<0.05$, Two-way ANOVA, Bonferroni Post-test) (Fig. 14F).

FIGURES

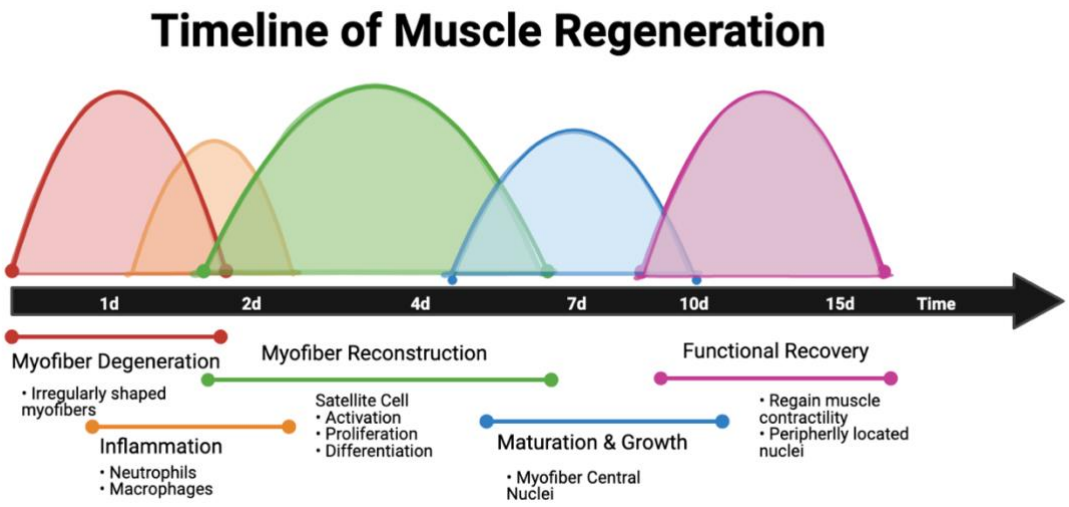

Figure 1. Model of Muscle Regeneration Timeline Under Healthy Conditions. Muscle regeneration occurs in 5 time-dependent and inter-related phases; myofiber degeneration, immediately accompanied by an inflammatory response, then myofiber reconstruction, maturation and growth of newly formed or repaired myofibers, and lastly function recovery (Forcina et al., 2020).

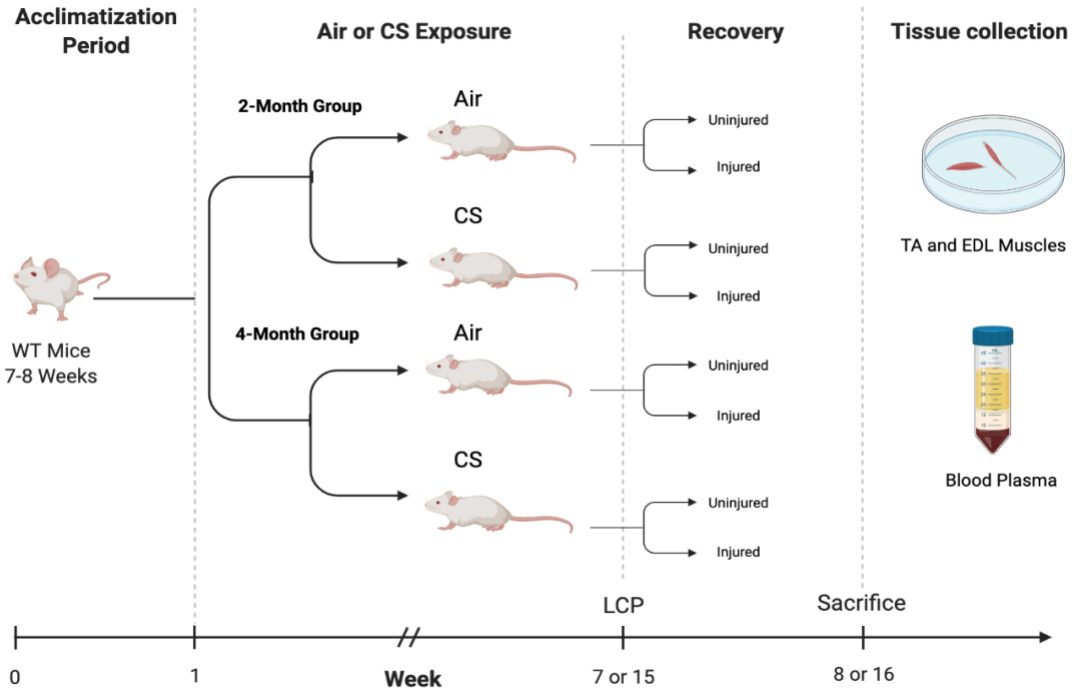

Figure 2. Experimental Overview of Air and CS Exposure Periods. Young adult (age 7-8 weeks) WT mice underwent 5-day acclimatization period before being randomly spilt up into 2- or 4-month exposure groups. Each group consists of Air and CS exposed mice, n=12 each. One week prior to the end of their exposure period the mice are subjected to a muscle injury (LCP). Of the hind limb muscles, one leg served as the uninjured control leg, while the other is the LCP leg. At the end of the exposure period, mice were sacrificed, and tissues were collected**.**

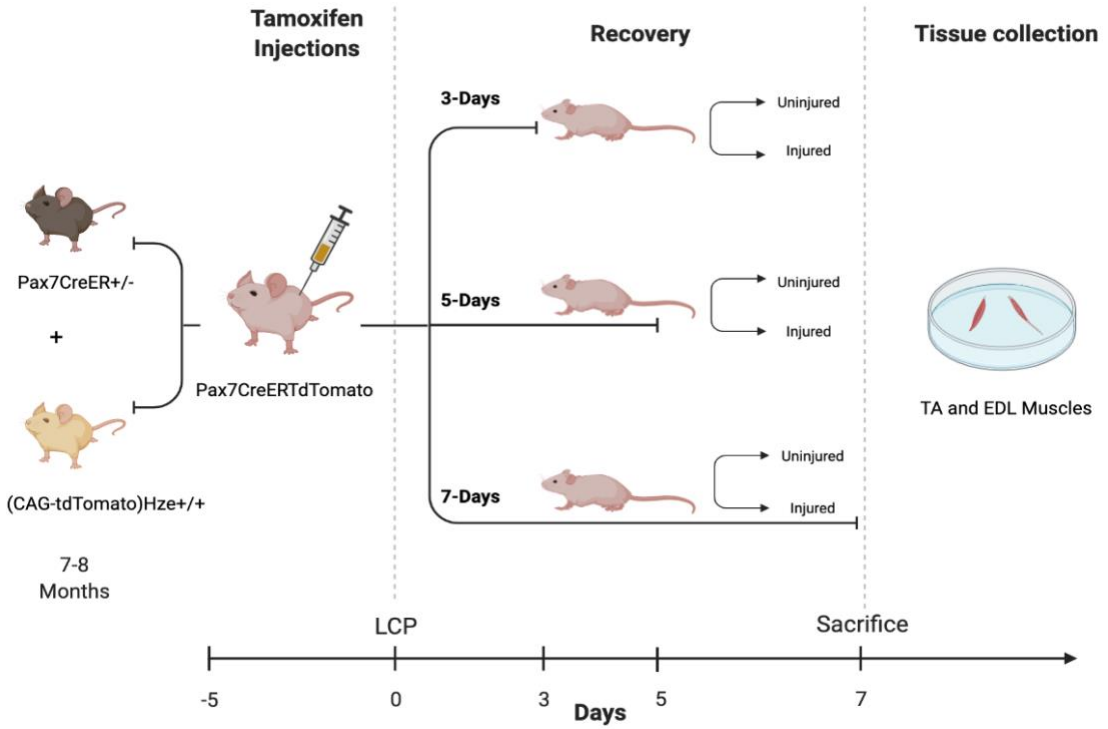

Figure 3. Experimental Overview of Pax7CreERTdTomato (Pax7TdT) mice 3-, 5-, 7-days recovery period. Male and female Pax7CreER+/- mice were crossed with B6.Cg-Gt(ROSA)26Sortm9(CAG-tdTomato)Hze/J+/+ to yield Pax7CreERTdTomato. At ages 7-8 months, mice were treated for 5-days with Tamoxifen injections to activate Pa7 expressing cells. Immediately following injections these mice were subjected to muscle injury, LCP, and split into three groups 3-day, 5-day, and 7-days recovery, of n=3 mice each. At the end of recovery TA and EDL muscles were collected.

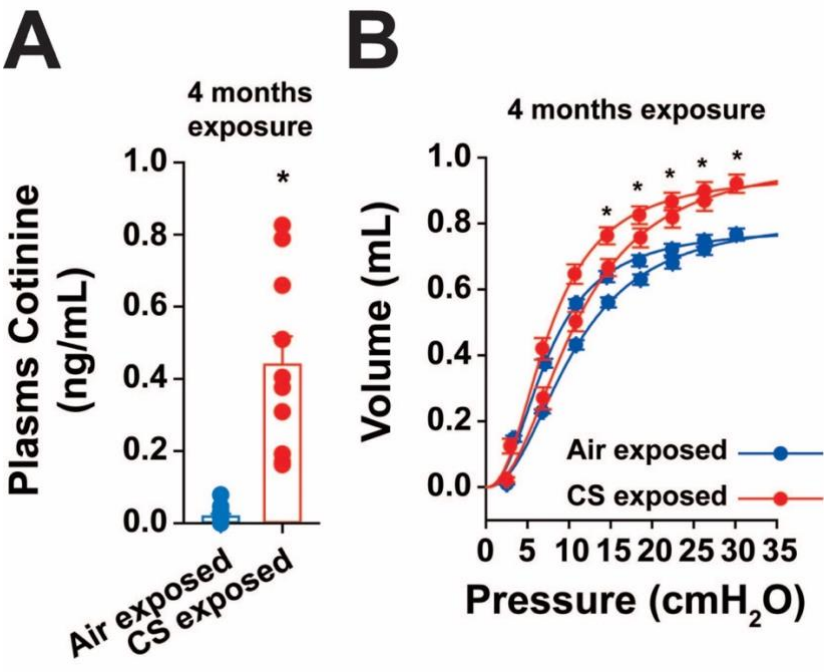

Figure 4. Cigarette Smoke Exposure validated by changes in lung mechanics and plasma cotinine levels. A) Plasma cotinine levels show in 4-month Air and CS exposed groups (n=12) ($P<0.0001$, T-test) B) Static lung mechanics was measured in 4-month Air and CS exposed mouse lungs in situ. Lung pressure-volume relationship of 4-month cigarette smoke exposed mice shows higher lung volume. Air (n=11), CS (n=8), ($P<0.0001$, Two-way ANOVA, Bonferroni post-test). Data are shown as Mean ± SE.

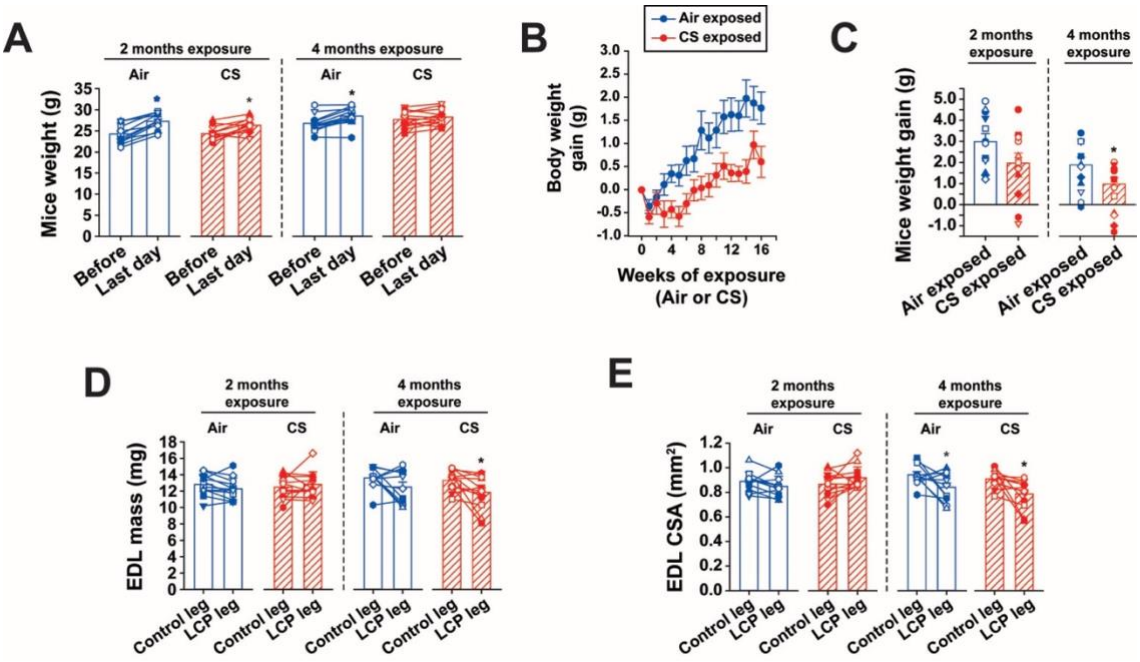

Figure 5. Changes in mouse weight and EDL muscle morphometrics in mice exposed for either 2 or 4 months with CS or Air. A) Body weight of mice measured before 2-month or 4-month exposure and on the last day of exposure. *P<0.05 vs Before, paired t-test; B) Mouse body weight (g) recorded weekly throughout duration of 4-month exposure period of Air and CS groups (n=12 mice each group). *P<0.05 vs Air exposed, t-test; C) Mouse body weight gain (g) reported as comparison from initial weight before and after 2 and 4-month exposure periods. D) Extensor digitorum longus (EDL) muscle mass (mg) and cross-sectional area (CSA) (mm2) E) from 2 and 4-month exposure groups (n=10-12) of LCP, injured, leg and contralateral, control, leg). *P<0.05 vs control leg, paired t-test. Data are shown as Mean ± SE

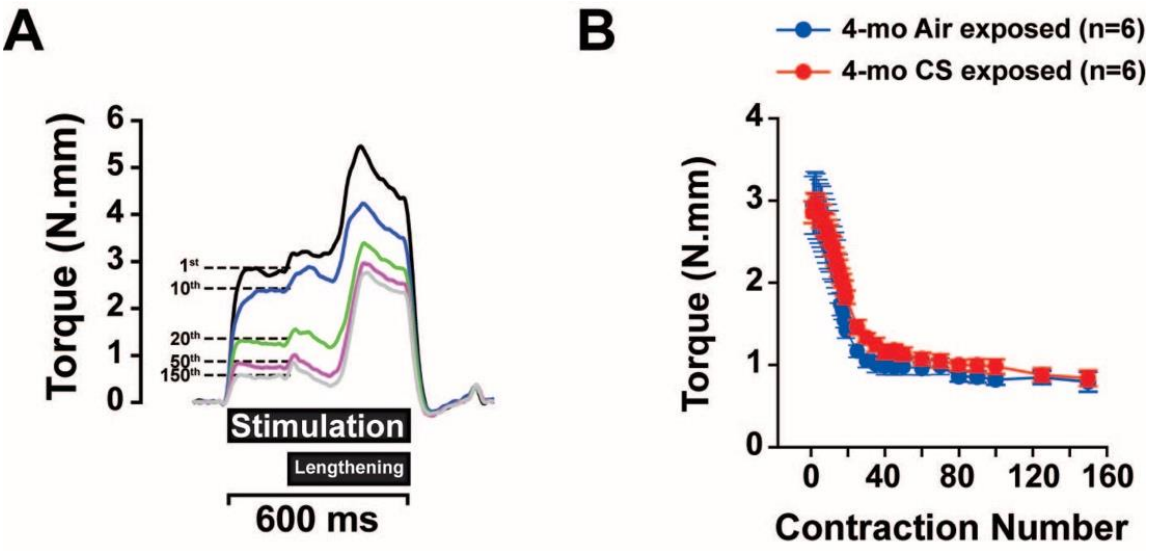

Figure 6. Lengthening contraction procedure (LCP) effectively decreases isometric dorsiflexion torque development in CS and Air Exposed mice anterior crural muscles. A) Averaged trace recordings of torque developed at different contractions (1st, 10th, 20th, 50th and the last contraction [150th]) during LCP in the air-exposed mice group. Peroneal nerve stimulation lasts for a duration of 600ms, after 200ms of isometric contraction active plantar flexion, "Lengthening" of the anterior crural muscles is induced by the motor lasting the remaining 400ms. B) Gradual decrease in peak isometric torque measurements during the LCP for both groups of 4-month exposed mice (Air or CS). Two-way ANOVA showed that curves are statistically different (P=0.011). Data are shown as Mean ± SE.

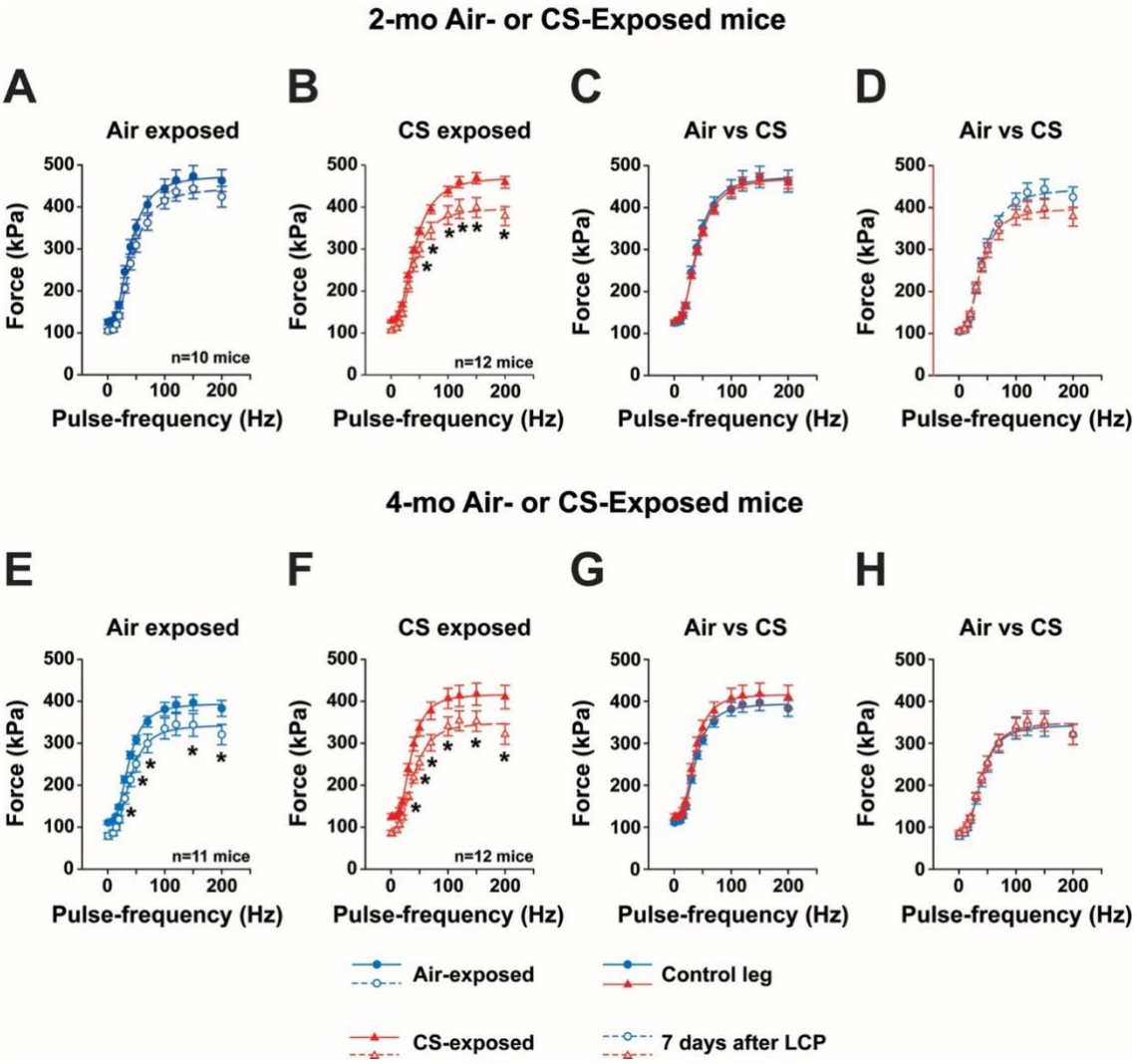

Figure 7. Changes in muscle force development of CS Exposed mice in isolated EDL during ex-vivo electrical stimulations 7 days after LCP. Effects of 2 months (Air n=10, CS n=12) (A-D) or 4 months (Air n=11, CS n=12) (E-H) of Air or CS exposure on isometric force development evoked by increasing frequencies of stimulation in EDL muscles dissected from control legs (closed symbols) and from LCP legs (open symbols). *P<0.05 vs control leg, Two-way ANOVA, repeated measures, Bonferroni post-test. Two-way ANOVA found that curves on panels A (P<0.0001), Control vs. LCP, D (P<0.05) and G (P<0.01) Air vs. CS are statistically different. Data are shown as Mean ± SE.

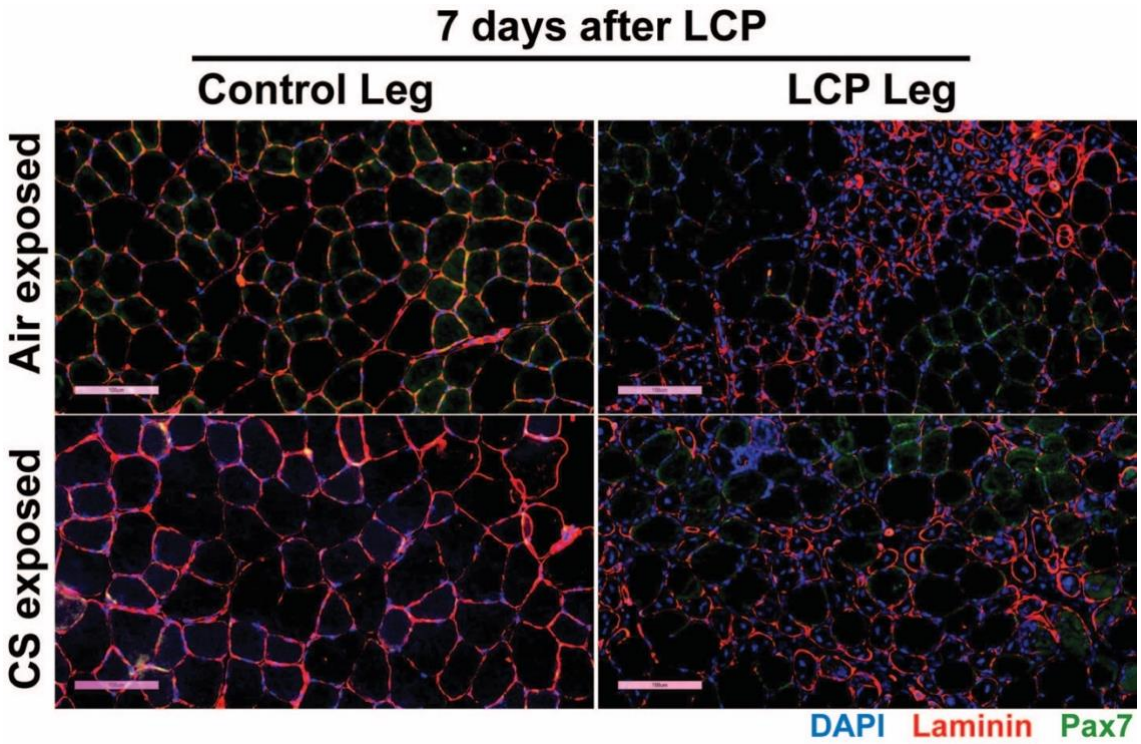

Figure 8. Effect of Cigarette Smoke exposure central nuclei+ myofibers of TA muscles one week after LCP injury. Immunofluorescent staining of cross-sectioned TA muscles 7-days post LCP injury, and contralateral uninjured leg, Control or Air exposed and CS exposed: Laminin (red), Pax7+ cells(green), and nuclei are stained with DAPI (blue). Scale bars represent 100μm^2

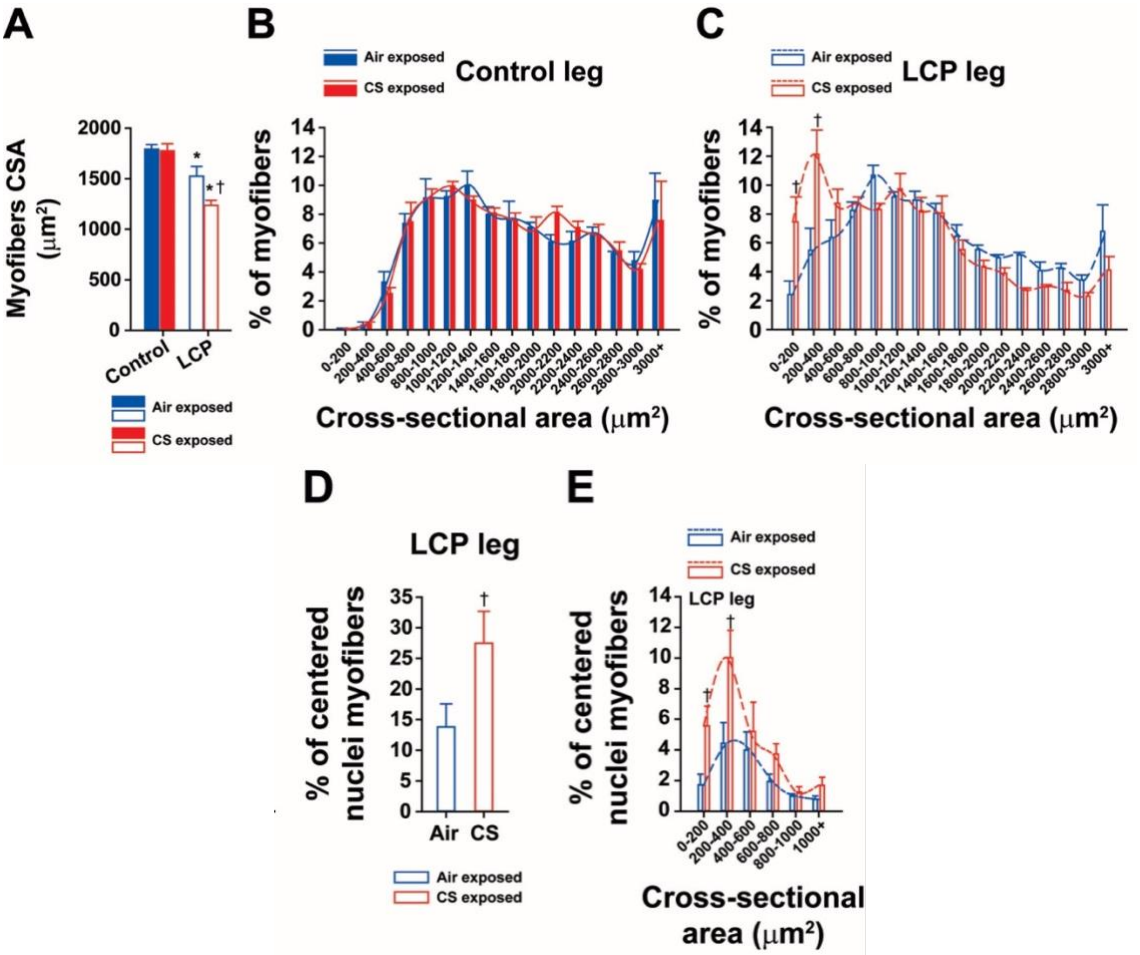

Figure 9. 4-month CS Exposure promotes Tibialis Anterior (TA) muscle wasting one week after induced eccentric muscle injury. A) Average myofiber cross-sectional area (CSA) from 10 μm histological sections of TA from both LCP and uninjured contralateral (control) legs *P<0.05 vs control, paired t-test; †P<0.05 vs LCP Air exposed, t-test; B-C) Distribution of myofibers CSAs shows that myofibers from CS exposed mice have a higher proportion of myofibers with a smaller CSA in LCP subjected hind limb †P<0.001 vs Air exposed, two-way ANOVA; D) Number of centered nuclei myofibers relative to total number of myofibers in the TA sections from LCP legs †P<0.05 vs Air exposed, t-test; E) Distribution of centered nuclei myofibers per total number of myofibers †P<0.01 vs Air exposed, two-way ANOVA. Mean ± SE, n=4 mice each.

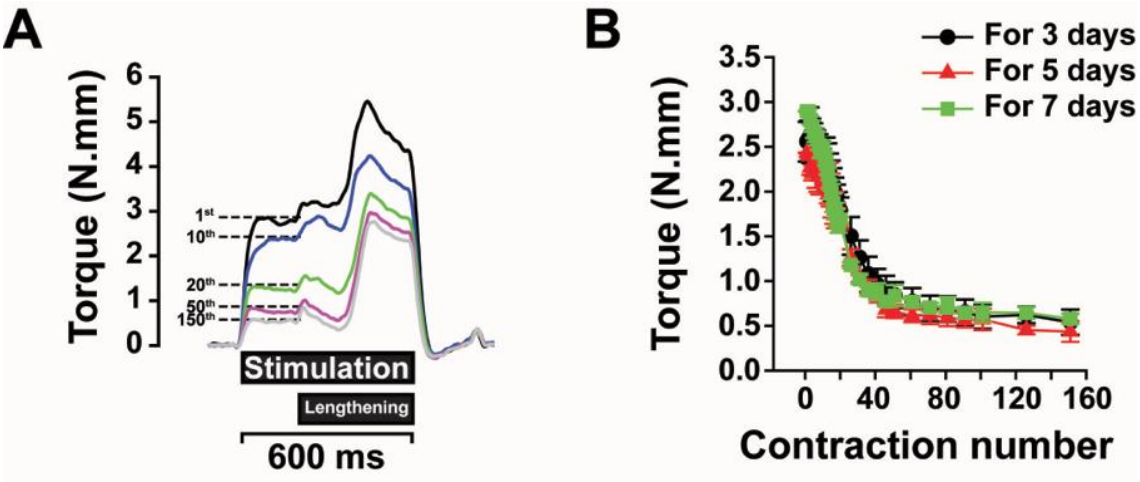

Figure 10. Lengthening contraction procedure (LCP) effectively decreases isometric dorsiflexion torque development in Pax7CreERTdTomato mouse anterior crural muscles. A) Averaged trace recordings of torque developed at different contractions (1st, 10th**,** 20th, 50th and the last contraction [150th]) during LCP. Dashed lines indicate the isometric phase of muscle contraction during nerve stimulation. B) Effects of LCP on isometric torque developed by the anterior crural muscles for the three groups (3d, 5d, 7d post-LCP) of mice. Mean ± SE, n=3 mice each group.

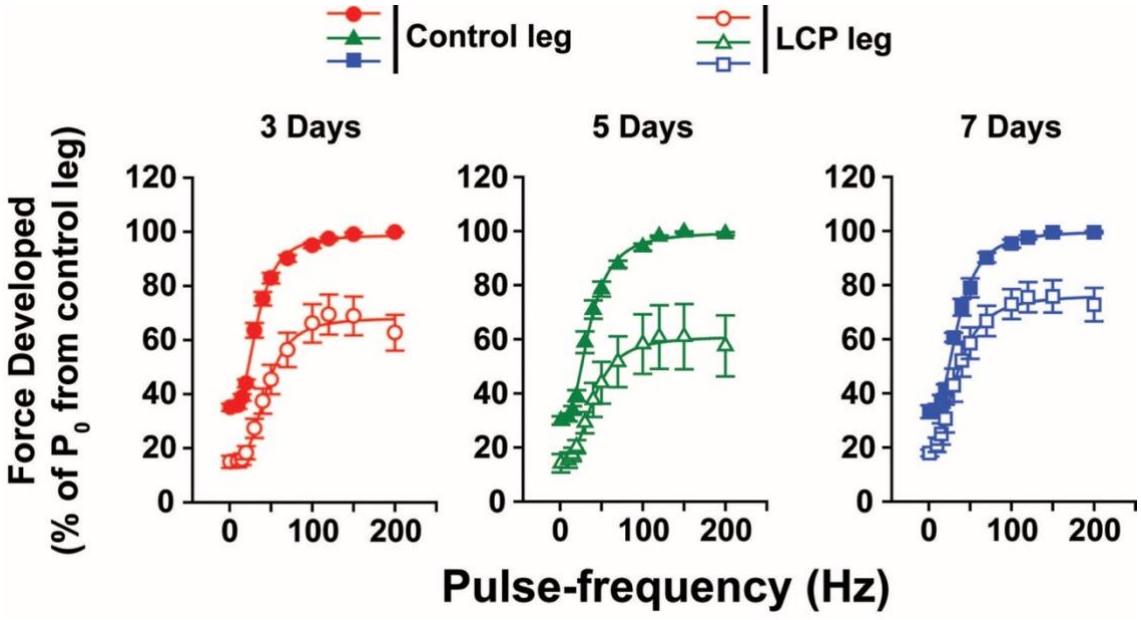

Figure 11. Isometric force developed by EDL muscles 3, 5 or 7 days after LCP. Force was normalized by the maximal tetanic force developed by the EDL muscle from the contralateral leg (control leg). Control leg force measurements from all 9 mice were averaged. Mean ± SE, n=3 mice each group. Two-way ANOVA shows that recoveries are different from 3-day to 7-day ($P<0.05$) and 5-day to 7-day ($P<0.05$).

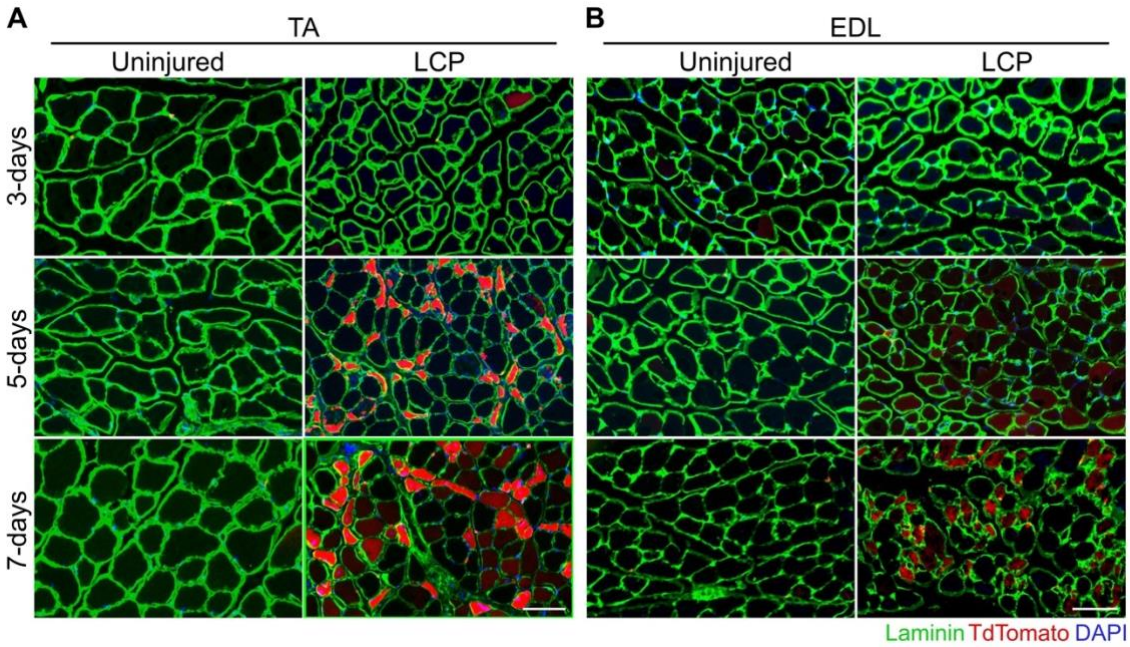

Figure 12. **Representative fluorescence images of TA (A) and EDL (B) muscle sections (10x) from mice recovered from LCP for 3 days, or 5 days or 7 days**. Contralateral legs (uninjured) from respective mice are shown. Green: anti-laminin; Blue: DAPI; Red: TdTomato.

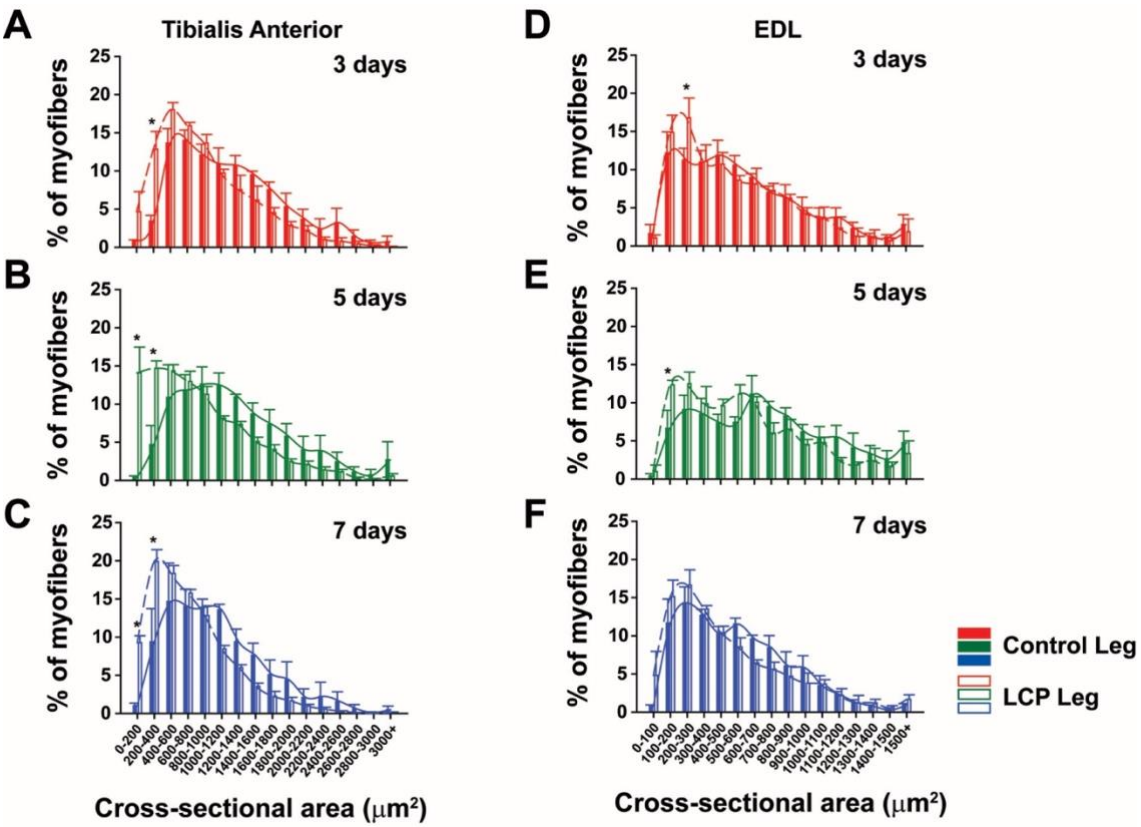

Figure 13. Effect of LCP on CSA distribution of TA (A, B, C) and EDL (D, E, F) muscles 3 days (A, D), 5 days (B, E), and 7 days (C, F) post-LCP. Quantification of CSA distribution are represented as a histogram with the % of myofibers per category. Open bars are LCP legs and closed bars represent contralateral (non-injured) control legs. *P<0.05 vs. control leg, two-way ANOVA.

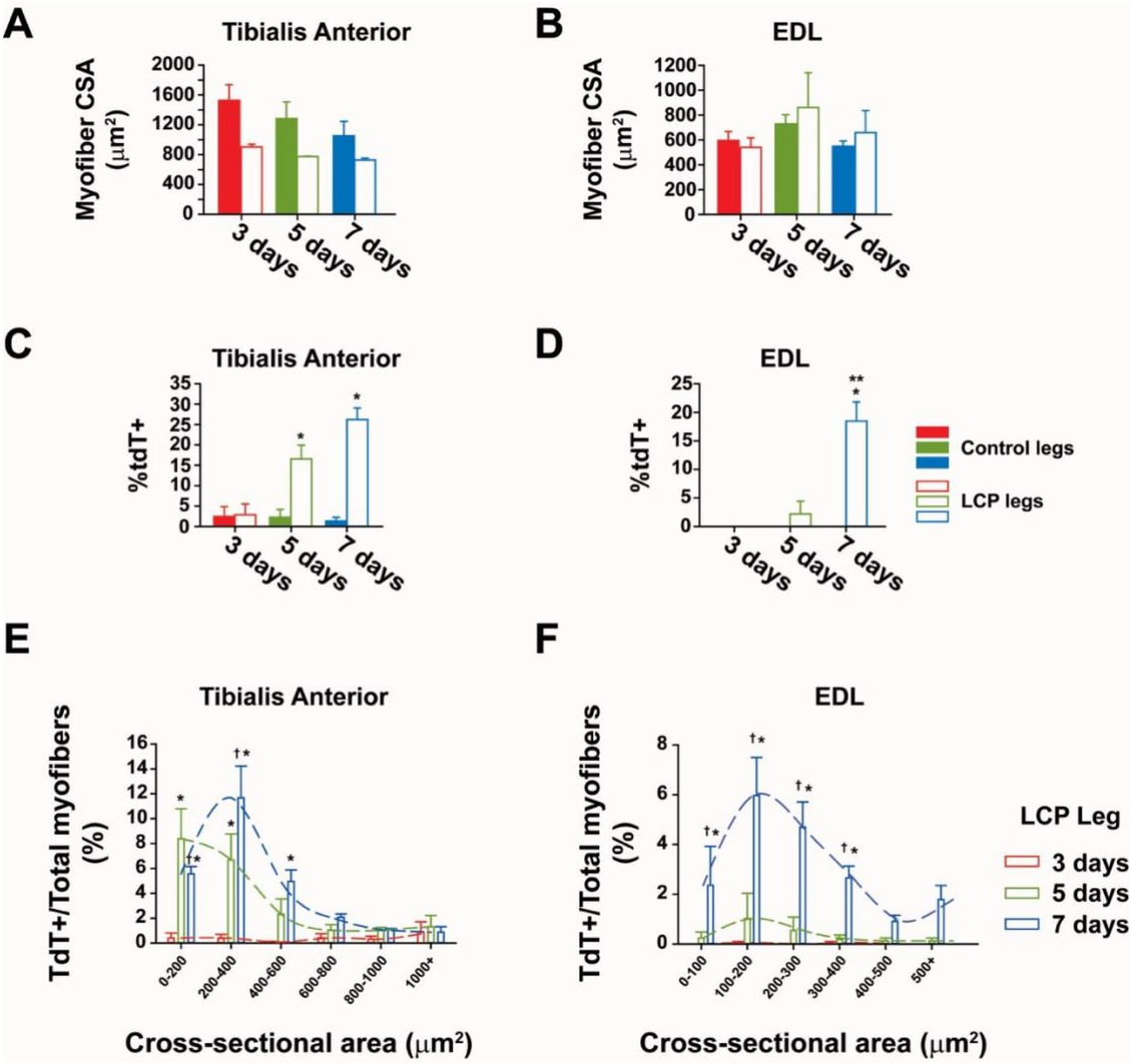

Figure 14. CSA of Td+ Myofibers and average Myofiber CSA of TA and EDL 3, 5, 7-day post LCP. Average of myofiber CSA from TA (A) and EDL (B) muscle sections. C-D) Number of myofibers positive to tdTomato fluorescence relative of total number of myofibers (%tdT+) in TA (C) and EDL (D) muscle sections. Open bars are LCP legs and closed bars represent contralateral (non-injured) control legs. *P<0.05 vs. 3 days, **P<0.05 vs. 5 days, two-way ANOVA. CSA of TdT+ myofibers from Tibialis Anterior muscle (A) and EDL muscle (B) at either 3, 5 or 7 days after LCP, relative to the total number of myofibers (1014 ± 61 myofibers for TA and 513 ± 19 myofibers for EDL) *P<0.05 vs 3 days; †P<0.05 vs 5 days, Two-way ANOVA, Bonferroni Post-test. Mean ±SE, n=3 mice each

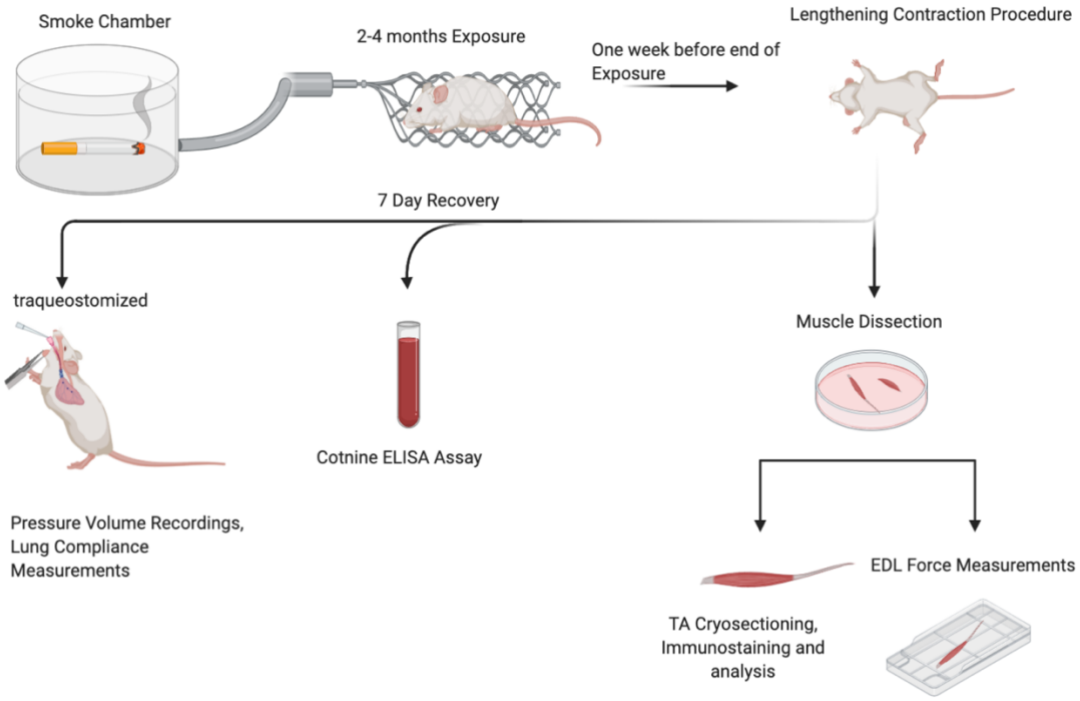

Figure 15. Overview of Nose-Only Cigarette Smoke Exposure System. Un-filtered research grade tobacco cigarettes were placed into a smoke chamber, a pump applied negative pressure to simulate a smoke puff. Smoke was delivered and distributed evenly to each mouse in the exposure system. One week prior to end of exposure period, mice undergo LCP procedure. After 7-days of recovery mice are traqeostomized for assessment of lung mechanics, blood plasma is collected for Cotinine assay, and muscle tissues are dissected.

DISCUSSION

The hypothesis of this study was that CS exposure would decrease the muscles' ability to repair one week after overuse injury. This was evaluated by skeletal muscle ex-vivo force contractility, myofiber CSA and regeneration after one-week recovery from an exercise induced injury. Additionally, we sought to investigate the amount of damage induced by the LCP method in anterior crural muscles (TA and EDL). Pax7CreERTdTomato (Pax7TdT) transgenic mice were used to better understand the relationship between the anterior crural muscles' regeneration process throughout at one-week recovery period by their expression of fluorescent protein TdTomato in Pax7 cells and in regenerating myofibers. This study was the first to investigate muscle repair with a method of muscle injury that is most analogous to what a patient is likely to experience. We modeled this in mice exposed to CS under pre-COPD like conditions.

Effects of CS on Lung Mechanics in Pre-COPD Mice

It has recently been suggested that skeletal muscle dysfunction exists in non-symptomatic smokers prior to the development of overt respiratory problems associated with COPD. Therefore, to study the early impact on muscle dysfunction in mice, multiple parameters were measured to assess the severity of pulmonary effects. Such parameters often considered include inflammatory cell counts of the lungs, the systemic inflammatory response, and the effects on lung mechanics via the pressure-volume relationship. A review on smoking-induced skeletal muscle dysfunction describes that

skeletal muscle weakness is present in CS exposed animal studies prior to the onset of respiratory problems (Degens et al., 2015).

Once we validated smoke exposure parameters, lung mechanics were measured in-vivo as lung airways were inflated and deflated. As anticipated, we observed a slight increase in the lung volumes of the 4-month CS exposed mice when compared to the air exposed mice. Previous research done by division colleagues (Ellen Breen Lab) validated this slight increase in lung volume may be attributable to CS-induced apoptosis of the alveolar wall structure or an increase in protease activity beginning to take place after 4-month CS exposure (Lee et al., 2019). This change in lung volume indicates the early stages of the lung mechanics being affected within the CS exposed mice. Other research showed development of overt respiratory problems such as, lung emphysema, begin to present in the form of decreased lung elasticity after 3-months nose-only CS exposure (Rinaldi et al., 2012) and are fully developed in mice after 6-mo CS exposure (Seimetz et al., 2011). Exposure period duration of 2 or 4 months were chosen to create a comparison between mice that do not have observable effects on lung mechanics after 2-month CS exposure, and mice which are in the early stages of developing an overt respiratory pathology such as COPD, after 4-months CS exposure.

Force Development of EDL Following CS Exposure and 7-days Post-injury

The effects of CS on skeletal muscle force production have been studied and showed varying results depending on exposure duration and muscle type. To better understand what is expected to occur in skeletal muscles exposed to CS in the presence of an injury, we must first understand how uninjured muscles are affected by CS. In a previous study looking at the EDL and Soleus of the mouse hind limb after 3 and 6-

months CS exposure, they found differing results between these muscles. While neither of the muscles had any changes in muscle mass after 3 and 6-months exposure, the soleus muscle had lower force production after 6-months CS exposure, while the EDL muscle remained unchanged in force production (Rinaldi et al., 2012). Rinaldi's study attributes the different results to muscle type: the EDL is a fast-twitch glycolytic muscle, and the soleus a slow-twitch oxidative muscle (Rinaldi et al., 2012). A review evaluated evidence surrounding the presence of skeletal muscle dysfunction in non-symptomatic smokers described the general consensus among multiple studies was that skeletal muscles become weaker and less fatigue resistant with smoking duration. This suggests that CS exposure was directly contributing to the muscle dysfunction prior to the onset of respiratory problems. Previous research done by our lab highlighted the direct effects of CS on muscles by exposing mice to CS and by subjecting the mice to CS components for 2-months. Injecting the mice with CS components allowed us to bypass the pulmonary implications of smoke exposure and directly study the effects of CS on the peripheral muscles. From this, we found that after 2-months of either smoke exposure or exposure to smoke components, the EDL and soleus muscles showed a decrease in muscle fatigue resistance (in-situ measurements), and impaired force contractility from ex-vivo data (Nogueira et al., 2018).

After 2-months of Air or CS exposure there appeared to be no change in force production of the uninjured control legs at this time. Which suggests that 2-months of nose-only CS exposure does not have an effect on the muscle's functionality, specifically as it pertains to force contractility. Although, our data showed a decrease in force production of the EDL in the 2-month CS exposed LCP legs when compared to

the Air LCP legs, this trend is not repeated in the 4-month exposed mice LCP legs. There appeared to be no significant difference between the Air and CS LCP legs of the 4-month mice, however, we did see a general decrease in force of the LCP legs when compared to the uninjured legs, in both Air and CS exposed mice. This result may be, in part, attributable to the overall decrease in force production seen in all 4-month mice. While the difference in force production between the 2- and 4-month mice is not statistically significant, we speculated that the restrictive conditions the mice are under demanded by the exposure protocol has a greater impact on the 4-month group since they are in these conditions 2 months longer than the 2-month exposed group of mice. This speculation was supported by our data showing that the body weight of the mice throughout the exposure periods (Figure 5) was different. Our data showed that the 2- and 4-month groups experienced significant weight attenuation, and this was found to be more prominent in the 4-month group of mice. The prolonged weight attenuation in overall body weight the 4-month group of mice experienced was likely a contributing factor to force production and that the confined experimental conditions the mice were placed under affected the muscles' ability to produce force. While overall body weight gain was attenuated in both 2- and 4-month groups of mice, a decrease in EDL muscle mass was only observed in the 4-month CS mice. Previous work from other teams has observed weight changes, specifically of the mouse hind limb muscles, only after 6 months of CS exposure (Krüger et al., 2015). Considering this, the decrease in EDL muscle mass observed only in our 4-month CS exposed mice, suggests that the main contributing factor would be that CS impacted the muscles' growth post-injury. Previous research suggests that the main indicator of muscle strength relies on the size

of the muscle, while capillary density, oxygen delivery, and metabolic factors of the myofibers contribute to a lesser extent (Barreiro & Gea, 2016). It is likely that the restrictive experimental conditions impaired muscle growth thus contributing to muscle weakness which may have masked any potential differences in force production across Air and CS exposure conditions.

While the experimental conditions seem to have an impact on the mice, the extent to which muscle damage has been induced to the muscle should be the main factor to consider. Our investigation first measured the torque produced by the anterior crural muscles to ensure the procedure was sufficiently implemented. This data showed a decrease in force of about 80% by the end of the procedure, which suggested 20% of the muscle remains capable of producing force. While torque measurements are a useful indicator of procedure implementation, we are not able to determine how much of the decrease in torque during the procedure was due to muscle fatigue versus muscle damage. Data gathered from the Pax7TdT mice revealed that after 7-days of recovery, about 18% of the EDL muscle fibers are in the peak of the reconstructive phase of muscle regeneration. This was evident by the amount of TdT positive fibers, ~18%, present 7-days after injury. Considering the data from the Pax7TdT mice, we were able to deduce the EDL in the Air or CS 4-month exposed mice endured a similar amount of damage and the muscle fibers are in the peak regenerative phase 7-days post-injury. This would suggest that the lack of severity of the damage induced to the muscle has resulted in a significant decrease in force production one week after injury, but this has not been exacerbated by the presence of CS after 4-months exposure.

Cigarette Smoke Exposure Delays Early-Stages of TA Muscle Regeneration

Previous research studying the effects of CS on muscle fibers presents some conflicting results as to when these changes occur. As previously mentioned, muscle fiber type composition plays a key role in the time course of these modifications. One study looking at the effects on muscle fiber-type shift and CSA after 2-, 4-, 6-, and 8-months CS exposure, found varying results in different murine hindlimb muscles. Indeed, they have shown a shift from slow (fiber type-1) to fast-twitch (fiber type-2) fibers after 6-months of CS exposure. Similar to this, a decrease of the muscle fiber CSA was observed in fast-twitch muscle fibers starting at 2-months CS exposure whereas decreased myofiber CSA observed in slow-twitch fibers were not significant until 8-months of smoke exposure (Krüger et al., 2015). Research done by division colleagues has found that changes in fiber type proportions, from type 2A (fast-oxidative) to type 2B (fast-glycolytic), was detected in the soleus muscle after 2-months of CS exposure and more pronounced after 4-months, while no changes were detected in the EDL (Tang et al., 2010). A change in muscle fiber types from slow- to fast is an established trait of chronic smoking and in those who have fully developed COPD, while it remains unclear why this occurs, we do know that fast-twitch glycolytic fibers (type-2B and 2x) have decreased time to fatigue (Talbot & Maves, 2016). Less fatigue resistant muscles are likely to cause problems for chronic smokers and COPD patients as this will impact their quality of life and ability to perform daily tasks, such as walking.

Skeletal muscle injury is often classified according to physiological or morphological indications, a typical assessment of muscle injury looks at muscle force

contractility, mentioned above, and structural changes of the myofibers. These parameters considered together provide valid information to assess muscle injury (Tidball, 2011). Following an injury, such as EEIMI, regeneration occurs in two main stages, deconstruction, and reconstruction. While the muscle regeneration process is heavily dependent on the severity of the damage induced, these phases are all interrelated and identifiable by certain characteristics (Forcina et al., 2020). Such characteristics can be seen through histological analysis of the muscle looking for architectural changes of the muscle fibers and the presence of cellular markers. Tissue deconstruction entails degeneration of myofibers accompanied by an inflammatory response, which is often observable by compromised myofiber CSA. Subsequently, the inflammatory response triggers the regenerative phase, which consists of satellite cell (SC) activation, expansion, and differentiation, this phase can be detected by the presence of the satellite cell-marker Pax7. A hallmark sign of this phase also includes the presence of centrally located nucleus withing the myofibers. Next, comes tissue reconstruction, evident by gradual restoration of myofiber CSA. The latter stages of muscle regeneration involve myofiber maturation and growth, this is complete once the nuclei have returned to its periphery and complete function has been regained (Forcina et al., 2020).

Currently, there is no research on the effects of myofiber atrophy following an injury after 4-months CS exposure. Data from our histological analysis of the TA muscles of the 4-month group, reveal that the control legs of the Air and CS exposed mice showed signs of healthy muscle tissue: myofibers were uniform in size evident by myofiber CSA with peripherally located nuclei. Whereas in the LCP legs of the Air and

CS exposed mice, damage was evident by irregularly shaped myofibers and the presence of central nuclei. As expected, the averaged myofiber CSA was significantly reduced in both Air and CS LCP legs and far more reduced in the CS exposed LCP legs 7-days after injury. Our data shows that the CS LCP legs have far more myofibers with CSA less than 1000 μm^2, and that the majority of these myofibers contain central nuclei. Data showing a far higher presence of myofibers containing centered nuclei indicate the muscle is recruiting more SCs to regenerate. As the SCs become activated and proliferate they fuse or create new myofibers in the form of myotubes in effort to repair the damaged area. Interestingly detected, is the presence of a higher number of central nuclei positive myofibers in the CS exposed LCP legs. This would suggest that CS has an effect on the regenerative phase of muscle repair. Further investigation is needed in order to determine the extent to which CS is affecting the muscle healing process and the stage that is affected most.

The use of Pax7TdT transgenic mice show the activation and incorporation of the Pax7 positive SCs into the myofibers. From this, we were able to see the healing process 3-, 5-, and 7-days following the LCP. In each of the 3, 5, and 7-day groups, there is a significant decrease in averaged myofiber CSA which correlates inversely to the rise in the presence of TdT positive myofibers during this time. This follows the expected timeline of the muscle regeneration process as we know it. Within the first few days following injury, activation of muscle regeneration begins, which includes the increased number of Pax7 positive SCs. Next, they will incorporate into the myofibers, which is what we were able to quantify by using the Pax7TdT mice since myofibers start to express fluorescent TdT. Later stages involve myofiber growth and maturation,

and lastly regain of function. The presence of central nuclei positive myofibers in the Air and CS mice closely correlates with the percentage of TdT positive myofibers after 7-days recovery. Our results suggests that the muscles are in a highly regenerative state 7-days after EEIMI, thus validating our method of injury and ensuing that CS delays the muscle regeneration process.

All things considered our data has indicated that while the LCP method of injury does induce enough damage to reduce force within a week following injury, evident by Pax7TdT mice, this was not a sufficient amount of damage to outweigh the experiment restrictions imparted on the 4-month Air or CS exposed mice. The higher presence of central nuclei positive myofibers in the 4-month CS exposed TA muscle supports the notion that CS influences the muscle's ability to regenerate, and possibly indicates that the muscle is trying to overcompensate in the presence of CS. In this newer area of research investigating whether CS has an effect on muscle regeneration there are important experimental procedures to consider in order to compare these results with other studies, such as the smoke exposure system, injury method, measurement of muscle force, and the muscles analyzed. The only other study done exploring the effects of CS following muscle injury shows that mice have a decrease in force production of the TA after 2-months CS exposure and one-week following muscle chemical injury (Chan et al., 2020). First off, the Chan et al. study used $BaCl_2$ as the method of muscle damage which induces a far greater amount of damage, however, this is not considered a physiological method of muscle injury. Also, their smoke exposure system places mice in a whole-body system, while the control, sham, mice were left in the vivarium not under the same stress conditions the CS exposed group endured. The smoke

delivery system used in our study implements a nose-only exposure to ensure each mouse is equally exposed to the same amount of smoke particles and for the same duration. Furthermore, our Air exposed group of mice were under the same restrictive conditions as the CS exposed mice, and they were not left in the vivarium at liberty to eat and drink during the 3 hours daily exposure periods that occurred 5 days a week. Lastly, Chan et al. evaluated the force of the TA under in-situ conditions, while we performed ex-vivo measurements of the EDL force, the former method includes conditional variables, which are not present in ex-vivo muscle contractility measurements. The more refined experimental approach of using the LCP method to induce physiologically relevant damage in addition to the fact that our control, Air exposed, mice underwent the same experimental conditions as the CS exposed mice, are likely the main contributing factors towards the lack of notable change in force production following 4-months CS exposure.

Future experiments would use either a revised more intense LCP method to induce damage or a more reliable yet less relevant method by injecting toxins to study this mechanism. The main limiting factor in this study would be the LCP method of damage, as it was not very severe, however, it was our priority to make this study as physiologically relevant as possible. Moving forward, with either the LCP method or damage induced by toxins, it would be useful to further investigate changes in the cellular markers present during the muscle regeneration process, such as number of Pax7 and MyoD positive satellite cells, and Myogenin expression. This can also be investigated at different time points such as 10-, 14-, or 21-days post-injury to see any potential long-term effects presented. The extent to which certain muscle fibers have

been affected by CS, with and without injury, would also be useful to investigate. This can be accomplished by measuring changes in the presence of certain fiber-types to determine if any fiber-type shift has occurred. From this, we would be able to measure the CSA of certain fiber types to see if some are more affected in the presence of CS and/or muscle injury. Identifying early changes in the muscle regeneration process, following a physiologically relevant method of damage, would be beneficial in the application towards prevention or treatment of chronic smokers and COPD patients as modeled in this experiment.

MATERIALS AND METHODS

Animals

Approval of this study was granted by UCSD Institutional Animal Care and Use Committee (IACUC) (protocol #S00250). Two strains of mice (male C57Bl6/J wild-type [WT] from Jackson Labs and, male and female Pax7CreER+/- crossed with B6.Cg-Gt(ROSA)26Sortm9(CAG-tdTomato)Hze/J+/+ [Pax7CreERTdTomato] kindly donated by Dr. Alessandra Sacco [Sanford Burnham Prebys Medical Discovery Institute] and bred at the UCSD vivarium) were used in the experimental procedures. Mice were housed with 3-4 per cage, in a 12 h:12 h day–night cycle and provided standard chow (Harlan Tekland 8604, Madison, WI, USA) and tap water *ad libitum*.

For the experiments in which mice were exposed to cigarette smoke (CS) (or air exposed), adult male WT (C57Bl/6J) mice, ages 7-8 weeks, were exposed for 2 or 4 months. Both 2 and 4-month groups of mice were used in the analysis of force production, while only the 4-month group of mice were included in the histological analysis. Mice were randomly assigned to Air-Exposed (control) or Cigarette Smoke Exposed (CS) groups (n=12 each). After 5 days of acclimatization in the nose-only exposure constraints, the mice began their 8 or 16-week exposure period, as outlined in Figure 15. The control mice were kept in the constraints on a water heated surgical pad at 37C° for the duration of the exposure to reduce confounding factors of stress, food and water intake, and body movement between the groups. Mice were weighed weekly to assess changes in body weight and health conditions.

Experiments were performed in male and female Pax7CreER+/- crossed with B6.Cg-Gt(ROSA)26Sortm9(CAG-tdTomato)Hze/J+/+ [Pax7CreERTdTomato] mice,

ages 7-8 months old. Mice were separated into three groups (3d, 5d, and 7d) groups (n=3 each). All mice were treated for five days immediately prior to muscle injury with tamoxifen to activate the expression of cre-recombinase only in Pax7 expressing cells (Pawlikowski et al., 2015) (2 mg/mouse/day, intraperitoneal injections (IP). On the last day, the right leg was subjected to a lengthening contraction procedure (LCP), while the contralateral leg was used as the control.

At time of mouse euthanasia, mice were anesthetized using a mixture of ketamine (100 mg/kg) and xylazine (10 mg/kg) (IP), mice were euthanized by cervical dislocation, and tissues were dissected.

Cigarette Smoke Exposure

Mice were exposed to un-filtered 1R6F research cigarettes, purchased from Kentucky Tobacco Research and Development Center at the University of Kentucky (Lexington, KY, USA.) All mice, both CS and Air-Exposed groups, were restrained in SoftRestraints from SCIREQ that are made of nylon-coated stainless-steel wire. For the nose-only exposure system, "InExpose" system (SCIREQ, Montreal, QC, Canada), the CS was produced by a negative pressure pump set at 3L/min with the motor programmed in increments of 2 seconds of smoke and 58 seconds of air, this simulates a smoke "puff" and ensures safe delivery of smoke to mice. Mice receive smoke twice a day with a 30 min fresh air break halfway through exposure, resulting in a total of 10 cigarettes/day, 5 consecutive days/week for 2 or 4 months. One week before the exposure period ended mice were subjected to muscle injury, lengthening contraction procedure (LCP). Exposure was continued throughout the one-week recovery period.

Smoke exposure was assessed by measuring the amount of cotinine in the serum collected from each mouse by ELISA, (Cat# EA100902 OriGene).

Muscle Injury / Lengthening Contraction Procedure

All mice were anesthetized with isoflurane throughout the entire procedure. The knee of the right hindlimb was positioned at a 90º angle and securely fixed in place while the foot was attached to a moveable pedal connected to the torque transducer (model QWFK-8M, 25 in-ozs, Honeywell International Inc) and servo motor. Electrodes were placed on the peroneal nerve and electrically stimulated to evoke contractions of the anterior crural muscles, mainly consisting of the TA and EDL muscles, of the right leg. The ankle of the right hind limb was positioned at 90º to maintain muscles at optimal length (L_o). The peroneal nerve was electrically stimulated for 600ms (0.1 ms pulses, 150 Hz pulse-frequency), implementing active plantar flexion, "lengthening," in the last 400 ms of stimulation, with 12s intervals between contractions for 30 min (total of 150 contractions), while the contralateral leg serves as the uninjured Control leg. Confirmation of decrements in torque production throughout the procedure were measured via torque transducer.

Contractile Function "Skeletal muscle ex vivo contractility"

Both EDL and TA muscles of mouse hindlimbs were dissected under anesthesia (ketamine: xylazine, 10:1 mg kg−1, IP). EDL muscles from the injured (LCP) leg and contralateral Control (uninjured) leg were mounted in an experimental chamber (Model 1500A with a 402A force transducer, Aurora Scientific Inc., Aurora, ON, Canada) and electrically stimulated (S88X stimulator, Grass Technologies) using square-wave pulses

(16 V; EDL: 250 ms train duration, 0.5 ms pulses, 22°C; soleus: 500 ms train duration, 0.5 ms pulses, 28°C). Muscles were constantly perfused with Tyrode solution (121 mMNaCl,5mMKCl, 1.8 mM CaCl2,0.5 mMMgCl2, 0.4 mM NaH2PO4, 24 mM NaHCO3, 5.5 mM glucose, 0.1 mM EGTA, containing 25 μM d-tubocurarine) continuously bubbled with 95% O2–5% CO2 (final pH 7.4). Muscles optimal length (L_o) was determined with single twitches and muscles allowed to rest for 15 min. Contractile function was evaluated by stimulating the muscle at different frequencies (1–150 Hz) with 100s intervals. After the contractile protocol, EDL muscles were blotted dry and weighed, and whole muscle cross-sectional area (CSA) was calculated by dividing the muscle mass in (mg) by the L_o (in mm) multiplied by the density of the muscle (1.06 mg/mm^3). Force development was normalized with respect to the muscle CSA (kPa). Mice were excluded from data if the muscle was visually damaged during the dissection or if the muscle escaped from the chamber while testing force development.

Static Lung Mechanics

On last day of the exposure period, prior to euthanasia, mice were anesthetized (ketamine: xylazine, 10:1 mg kg−1, IP) then traqueostomized in vivo. Lung pressure-volume mechanical measurements were performed in situ in a FlexiVent (SciReq) to evaluate changes in lung mechanics. Airway pressures were measured as lung inflated in increments of 0.1 -mL until an airway pressure of 20 cm H20 was reached, then lungs were deflated.

Immunohistochemistry

All histological analysis was performed in muscle tissues embedded in optimal cutting temperature compound (O.C.T), flash frozen in isobutane and liquid nitrogen, and stored at -80 °C until sectioned to 10 μm thickness using the cryotome.

For histological analysis of CS and Air Exposed mice TA muscle sections were fixed with 4% PFA at room temperature (RT) for 15 minutes, blocked with diluted (1:10) AffiniPure Fab Fragment Goat Anti-Mouse IgG (H+L) (Jackson Labs) in PBST-B (1x PBS + 0.1% Triton-100 + 2% Bovine Serums Albumin) "blocking buffer" for 30 minutes at RT. Blocking buffer was removed and primary antibody solution (rat anti-laminin + rabbit anti-KI67) diluted in blocking buffer (1:100) incubated for 1 hour at RT, followed by 1-hour incubation of secondary antibodies Alexa rabbit 546 and rat 657 diluted in PBST-B (1:250). Sections were fixed again, heat activated antigen retrieval was performed to unmask Pax7 cells, slides were blocked again, and primary antibody solution diluted (1:100) in blocking buffer mouse anti-pax7 was incubated overnight at 4 °C. Followed by secondary antibody mouse Alexa 488. CSA samples were imaged with Inverted IX81 Olympus Compound Fluorescence Microscope at 20x magnification. Tissues were analyzed for CSA and central nucleated myofibers using FIJI software.

Experiments performed in Pax7CreERTdTomato mice TA and EDL muscle tissues were pre-fixed in 4% PFA for 2 hours on ice followed by 30% w/v sucrose treatment on ice overnight then flash frozen and cut. Sections were fixed with 4% PFA at RT for 10 minutes, blocked with PBST-B (PBS with 0.1% Triton-100 and 5% Bovine Serum Albumin, "blocking buffer") for 1 hour at RT, then incubated with primary

antibody solution. Primary antibody rabbit anti-laminin diluted (1:100) with blocking buffer, incubated overnight at 4 °C, secondary antibody goat anti-rabbit IgG (H+L) Alexa 488 diluted (1:250) with blocking buffer and incubated in dark for 1 hour at RT. Slides were mounted with Prolong Gold Antifade Mountant with DAPI and imaged with Inverted IX81 Olympus Compound Fluorescence Microscope. Images were taken at 10x magnification, 2 images taken for the TA and 1 for the EDL were used to analyze the CSA and TdTomato+ fibers. Cross-sectional area of the myofibers was measured by adjusting the brightness and contrast of the image and applying a threshold to the entire image. TdTomato+ fibers were determined by adjusting the brightness and contrast of the red channel so that most of the fibers that were red also contained central nuclei, the same parameters were

Statistical Analysis

For comparisons between two groups student t-test was used, as indicated. For comparisons between multiple groups, one-way ANOVA followed by the Tukey test or two-way ANOVA followed by the Bonferroni test was used, as indicated. Analyses were carried out using PRISM 4 software (GraphPad Software, La Jolla, CA, USA) and $P < 0.05$ was considered to represent a significant difference.

I would like to acknowledge Professor Michael C. Hogan for allowing me the opportunity to be a part of the lab in order to discovery my passion for research.

I would also like to acknowledge Leo, because none of this would have been possible without the creativity of your thinking to make this project happen. I have been so blessed to work alongside a P.I. as exciting as you.

To our grant collaborators at Sanford Burnham Prebys Medical Discovery Institute in Alessandra Sacco's Lab, I am so grateful to have had the opportunity to work with both Alessandra Sacco and postdoc Mafalda Loreti. Mafalda has served as a mentor to me throughout my graduate research, I would not have been able to accomplish so much of this project if it wasn't for her outstanding guidance and support along the way.

This manuscript is coauthored with Michael C. Hogan, Leonardo Nogueira, Alessandra Sacco, and Mafalda Loreti. The thesis author was the primary author of this manuscript.

REFERENCES

Agustí, A. G. N. (2005). Systemic Effects of Chronic Obstructive Pulmonary Disease. *Proceedings of the American Thoracic Society*, *2*, 367–370. https://doi.org/10.1513/pats.200504-026SR

Augusto, V., Padovani, C. R., & Rocha Campos, G. E. (2004). Skeletal muscle fiber types in C57Bl6J mice. In *Braz. J. morphol. Sci* (Vol. 21, Issue 2).

Barnes, P. J., & Celli, B. R. (2009). Systemic manifestations and comorbidities of COPD. In *European Respiratory Journal* (Vol. 33, Issue 5, pp. 1165–1185). European Respiratory Society. https://doi.org/10.1183/09031936.00128008

Barreiro, E., & Gea, J. (2016). Review Series Molecular and biological pathways of skeletal muscle dysfunction in chronic obstructive pulmonary disease. *Chronic Respiratory Disease*, *13*(3), 297–311. https://doi.org/10.1177/1479972316642366

Baumgarten, K. M., Gerlach, D., Galatz, L. M., Teefey, S. A., Middleton, W. D., Ditsios, K., & Yamaguchi, K. (2010). Cigarette smoking increases the risk for rotator cuff tears. *Clinical Orthopaedics and Related Research*, *468*(6), 1534–1541. https://doi.org/10.1007/s11999-009-0781-2

Chan, S. M. H., Cerni, C., Passey, S., Seow, H. J., Bernardo, I., Van Der Poel, C., Dobric, A., Brassington, K., Selemidis, S., Bozinovski, S., & Vlahos, R. (2020). *Cigarette Smoking Exacerbates Skeletal Muscle Injury without Compromising Its Regenerative Capacity*. https://doi.org/10.1165/rcmb.2019-0106OC

Chargé, S. B. P., & Rudnicki, M. A. (2004). Cellular and Molecular Regulation of Muscle Regeneration. *Physiological Reviews*, *84*(1), 209–238. https://doi.org/10.1152/physrev.00019.2003

Chen, H., Vlahos, R., Bozinovski, S., Jones, J., Anderson, G. P., & Morris, M. J. (2005). Effect of short-term cigarette smoke exposure on body weight, appetite and brain neuropeptide Y in mice. *Neuropsychopharmacology*, *30*(4), 713–719. https://doi.org/10.1038/sj.npp.1300597

CheungID, K.-K., Kai-Hang Fung, T., W Mak, J. C., Cheung, S.-Y., He, W., Leung, J. W., M Lau, B. W., & C NgaiID, S. P. (2020). *The acute effects of cigarette smoke exposure on muscle fiber type dynamics in rats*. https://doi.org/10.1371/journal.pone.0233523

Christov, C., Chrétien, F., Abou-Khalil, R., Bassez, G., Vallet, G., me Authier, F.-J., Bassaglia, Y., Shinin, V., Tajbakhsh, S., Chazaud, B., & Gherardi, R. K. (2007). Muscle Satellite Cells and Endothelial Cells: Close Neighbors and Privileged Partners □ D. *Molecular Biology of the Cell*, *18*, 1397–1409. https://doi.org/10.1091/mbc.E06

Degens, H., Gayan-Ramirez, G., & Van Hees, H. W. H. (2015). Smoking-induced skeletal muscle dysfunction: From evidence to mechanisms. In *American Journal of Respiratory and Critical Care Medicine* (Vol. 191, Issue 6, pp. 620–625). American Thoracic Society. https://doi.org/10.1164/rccm.201410-1830PP

Dueweke, J. J., Awan, T. M., & Mendias, C. L. (2017). Regeneration of skeletal muscle after eccentric injury. In *Journal of Sport Rehabilitation* (Vol. 26, Issue 2, pp. 171–179). Human Kinetics Publishers Inc. https://doi.org/10.1123/jsr.2016-0107

Dumont, N. A., Bentzinger, C. F., Sincennes, M. C., & Rudnicki, M. A. (2015). Satellite cells and skeletal muscle regeneration. *Comprehensive Physiology*, *5*(3), 1027–1059. https://doi.org/10.1002/cphy.c140068

Forcina, L., Cosentino, M., & Musarò, A. (2020). cells Mechanisms Regulating Muscle Regeneration: Insights into the Interrelated and Time-Dependent Phases of Tissue Healing. *Cells* , *9*(5). https://doi.org/10.3390/cells9051297

Gardner, T., Kenter, K., & Li, Y. (2020). *Fibrosis following Acute Skeletal Muscle Injury: Mitigation and Reversal Potential in the Clinic*. https://doi.org/10.1155/2020/7059057

Gosker, H. R., Langen, R. C. J., Bracke, K. R., Joos, G. F., Brusselle, G. G., Steele, C., Ward, K. A., Wouters, E. F. M., & Schols, A. M. W. J. (2009). Extrapulmonary Manifestations of Chronic Obstructive Pulmonary Disease in a Mouse Model of Chronic Cigarette Smoke Exposure. *American Journal of Respiratory Cell and Molecular Biology*, *40*(6). https://doi.org/10.1165/rcmb.2008-0312OC

Hardy, D., Besnard, A., Latil, M., Jouvion, G., Briand, D., Thépenier, C., Pascal, Q., Guguin, A., Gayraud-Morel, B., Cavaillon, J.-M., Tajbakhsh, S., Rocheteau, P., & Chrétien, F. (2016). *Comparative Study of Injury Models for Studying Muscle Regeneration in Mice*. https://doi.org/10.1371/journal.pone.0147198

Järvinen, T. A. H., Kääriäinen, M., Äärimaa, V., Järvinen, M., & Kalimo, H. (2008). Skeletal Muscle Repair After Exercise-Induced Injury. In *Skeletal Muscle Repair and Regeneration* (pp. 217–242). Springer Netherlands. https://doi.org/10.1007/978-1-4020-6768-6_11

Joaquim, G., Pascual, S., Casadevall, C., Orozco-Levi, M., & Barreiro, E. (2015). Muscle dysfunction in chronic obstructive pulmonary disease: update on causes and biological findings. *Journal of Thoracic Disease*, *7*(10), 418–438. https://doi.org/10.3978/j.issn.2072-1439.2015.08.04

Krüger, K., Dischereit, G., Seimetz, M., Wilhelm, J., Weissmann, N., & Mooren, F. C. (2015). Time course of cigarette smoke-induced changes of systemic inflammation and muscle structure. *Am J Physiol Lung Cell Mol Physiol*, *309*, 119–128. https://doi.org/10.1152/ajplung.00074.2015.-It

Leberl, M., Kratzer, A., & Taraseviciene-Stewart, L. (2013). Tobacco smoke induced COPD/emphysema in the animal model-are we all on the same page? *Frontiers in Physiology*, *4 MAY*. https://doi.org/10.3389/fphys.2013.00091

Lee, J. H., Hailey, K. L., Vitorino, S. A., Jennings, P. A., Bigby, T. D., & Breen, E. C. (2019). *ORIGINAL RESEARCH Cigarette Smoke Triggers IL-33-associated Inflammation in a Model of Late-Stage Chronic Obstructive Pulmonary Disease*. https://doi.org/10.1165/rcmb.2018-0402OC

Lovering, R. M., & Brooks, S. V. (2014). Eccentric exercise in aging and diseased skeletal muscle: good or bad? *Journal of Applied Physiology*, *116*(11), 1439–1445.

https://doi.org/10.1152/japplphysiol.00174.2013

Matsumoto, A., Ino, T., Ohta, M., Otani, T., Hanada, S., Sakuraoka, A., Matsumoto, A., Ichiba, M., & Hara, M. (2010). Enzyme-linked immunosorbent assay of nicotine metabolites. *Environ Health Prev Med*, *15*, 211–216. https://doi.org/10.1007/s12199-009-0129-2

Mauro, A. (1961). *SATELLITE CELL OF SKELETAL MUSCLE FIBERS*. http://rupress.org/jcb/article-pdf/9/2/493/1078104/493.pdf

Musarò, A. (2014). *The Basis of Muscle Regeneration*. https://doi.org/10.1155/2014/612471

Nogueira, L., Trisko, B. M., Lima-Rosa, F. L., Jackson, J., Lund-Palau, H., Yamaguchi, M., & Breen, E. C. (2018). Cigarette smoke directly impairs skeletal muscle function through capillary regression and altered myofibre calcium kinetics in mice. *Journal of Physiology*, *596*(14), 2901–2916. https://doi.org/10.1113/JP275888

Pauwels, R. A., Buist, A. S., Calverley, P. M. A., Jenkins, C. R., & Hurd, S. S. (2001). Global strategy for the diagnosis, management, and prevention of chronic obstructive pulmonary disease: NHLBI/WHO Global Initiative for Chronic Obstructive Lung Disease (GOLD) workshop summary. *American Journal of Respiratory and Critical Care Medicine*, *163*(5), 1256–1276. https://doi.org/10.1164/ajrccm.163.5.2101039

Pawlikowski, B., Pulliam, C., Betta, N. D., Kardon, G., & Olwin, B. B. (2015). Pervasive satellite cell contribution to uninjured adult muscle fibers. *Skeletal Muscle*, *5*(1). https://doi.org/10.1186/s13395-015-0067-1

Rinaldi, M., Maes, K., De Vleeschauwer, S., Thomas, D., Verbeken, E. K., Decramer, M., Janssens, W., & Gayan-Ramirez, G. N. (2012). Long-term nose-only cigarette smoke exposure induces emphysema and mild skeletal muscle dysfunction in mice. *DMM Disease Models and Mechanisms*, *5*(3), 333–341. https://doi.org/10.1242/dmm.008508

Seimetz, M., Parajuli, N., Pichl, A., Veit, F., Kwapiszewska, G., Weisel, F. C., Milger, K., Egemnazarov, B., Turowska, A., Fuchs, B., Nikam, S., Roth, M., Sydykov, A., Medebach, T., Klepetko, W., Jaksch, P., Dumitrascu, R., Garn, H., Voswinckel, R., Weissmann, N. (2011). Inducible NOS inhibition reverses tobacco-smoke-induced emphysema and pulmonary hypertension in mice. *Cell*, *147*(2), 293–305. https://doi.org/10.1016/j.cell.2011.08.035

Talbot, J., & Maves, L. (2016). Skeletal muscle fiber type: using insights from muscle developmental biology to dissect targets for susceptibility and resistance to muscle disease. *Wiley Interdiscip Rev Dev Biol.* https://doi.org/10.1002/wdev.230

Talukder, M. A. H., Johnson, W. M., Varadharaj, S., Lian, J., Kearns, P. N., El-Mahdy, M. A., Liu, X., & Zweier, J. L. (2011). Chronic cigarette smoking causes hypertension, increased oxidative stress, impaired NO bioavailability, endothelial dysfunction, and cardiac remodeling in mice. *American Journal of Physiology - Heart and Circulatory Physiology*, *300*(1), 388–396. https://doi.org/10.1152/ajpheart.00868.2010

Tang, K., Wagner, P. D., & Breen, E. C. (2010). TNF-α-mediated reduction in PGC-1α may impair skeletal muscle function after cigarette smoke exposure. *Journal of Cellular Physiology*, *222*(2), 320–327. https://doi.org/10.1002/jcp.21955

Tidball, J. G. (2011). Mechanisms of muscle injury, repair, and regeneration. *Comprehensive Physiology*, *1*(4), 2029–2062. https://doi.org/10.1002/cphy.c100092

Vogt, M., & Hoppeler, H. H. (2014). Eccentric exercise: Mechanisms and effects when used as training regime or training adjunct. In *Journal of Applied Physiology* (Vol. 116, Issue 11, pp. 1446–1454). American Physiological Society. https://doi.org/10.1152/japplphysiol.00146.2013